

# Identification of esters in carious dentine

Staining and chemo-mechanical excavation

Ulrica Scherdin-Almhöjd

Department of Cariology  
Institute of Odontology  
Sahlgrenska Academy at University of Gothenburg



UNIVERSITY OF GOTHENBURG

Gothenburg 2017

Cover illustration: A microscope picture of tooth stained by a hydrazine derivative (own analysis).

Identification of esters in carious dentine

© Ulrica Scherdin-Almhöjd 2017

[ulrica.almhojd@gu.se](mailto:ulrica.almhojd@gu.se)

ISBN 978-91-629-0069-4

Permission for reprinting has been obtained from Oral Health and Dental Management (Paper I and Paper II) and from Taylor & Francis journals (Paper IV).

Printed by Ineko AB, Gothenburg, Sweden, 2017

“Never give up on something that you can't go a day without thinking about”  
with the excuse to Winston Churchill

To Jonas, Emil and Noah



## ABSTRACT

Dental caries is clinically seen as a yellowish-brown discoloration that can be explained by the reactions between proteins and sugars resulting in Maillard products. However, the discoloration of carious dentine is an imprecise indicator of whether or not the dentine is caries free. Other processes might act in concert with the Maillard reactions. This thesis describes how special functional groups formed in the carious process can be used in connection with dyes that selectively stain the carious tissue in order to avoid over excavation.

The initial study aimed to analyse unique functional groups in sound and carious dentine and their presumed reaction with hydrazine derivative using Fourier Transform Infrared Spectroscopy (FTIR) and Time-of-Flight Secondary Ion Mass Spectrometry (ToF-SIMS). The second and third studies focused on the possible formation of covalent bonds between carious dentine and  $^{15}\text{N}_2$ -hydrazine,  $^{15}\text{N}_2$ -labelled Lucifer yellow, and stains carrying a hydrazine derivative respectively, using ToF-SIMS, solid-state NMR spectroscopy ( $^{13}\text{C}$  and  $^{15}\text{N}$ ) and light-microscopic observations. The latter aimed to evaluate the type of binding, electrostatic or covalent, to carious dentine. In a systematic review with an adjacent meta-analysis, the ability of a chemically based product in clinical caries excavation was evaluated by comparing the efficacy of chemo-mechanical excavation with that of traditional rotating instruments.

The results revealed ester groups unique to the carious dentine, with a higher occurrence in the inner layer of carious dentine, which, after reaction with hydrazine derivative, form covalent bonds not seen in sound dentine. This is a selective binding in comparison with dyes with only an electrostatic binding capacity. The systematic review found that the chemo-mechanical excavation technique is as efficient as burs, albeit with a longer treatment time but with enhanced patient comfort.

It is concluded that ester functional groups unique to carious dentine can be specifically stained with dyes carrying a hydrazine group, thereby acting selectively in distinguishing between sound and carious dentine. As a result, using a more precise indicator will support the identification of the end-point during clinical caries excavation.

**Keywords:** Caries detection, Carious dentine, Caries removal, Carisolv, Chemo-mechanical, Covalent binding, Dental caries, Electrostatic binding, FTIR, Hydrazine derivative, NMR, Staining, Systematic review, ToF-SIMS

# SAMMANFATTNING PÅ SVENSKA

Att kunna särskilja sjuk och frisk tandvävnad under operativ kariesbehandling utgör en svår gränsdragning och en anledning till varför en mer specifik detektionsmetod efterfrågas. En majoritet av infärgningsmetoderna är av elektrostatisk karaktär och går att tvätta bort samtidigt som de även verkar färga in opåverkat dentin. En specifik infärgning till kariös vävnad skulle kunna skilja denna från frisk. Några kariesunika strukturer, d.v.s. molekyllära enheter specifika för den kariösa vävnaden som sedan kan färgas, har hittills inte identifieras.

Syftet med detta avhandlingsarbete var att studera om det finns molekyllära förändringar som är unika för kariesvävnaden och om dessa kan detekteras. Därför har både karierat och friskt dentin renats fram och behandlats med olika substanser. Reaktionerna har därefter analyserats med ytkemiska instrument som infrarött ljus (FTIR), massupptagning (ToF-SIMS), strukturell teknik (NMR) och stereomikroskopi. Ett avslutande delarbete har i en systematisk utvärdering jämfört effektiviteten för avlägsnande av kariös vävnad av kemo-mekaniskt och borr.

Delarbete I visade att det fanns unika kemiska strukturer, esterfunktioner, endast i kariös vävnad. Dessutom fanns en högre förekomst av estrar i den inre delen av kariesangreppet. I delarbete II sågs att olika markörer har varierande förmåga att binda till kariös vävnad till skillnad från frisk vävnad. Samma arbete visade också att man kunde skilja mellan specifika och ospecifika markörer. Hydrazinbaserade markörer visade sig binda kovalent till estergrupper. Delarbete III visade att estergrupperna i karies kan reagera med isotopmärkt hydrazin vilket gav nya kemiska föreningar. Den systematiska genomgången av kliniska studier där kemo-mekanisk borttagning av kariös vävnad använts (delarbete IV) visade att kemo-mekanisk teknikologi är lika effektiv som roterande instrument för borttagning av karies.

Studien visar att det finns unika grupper, estrar, i karierat dentin som går att färga specifikt med hydrazinderivat, vilket underlättar gränsdragningen mellan frisk och kariös vävnad. Detta reducerar risken för onödig borttagning av frisk tandsubstans. Vidare har kemo-mekaniskt kariesavlägsnande visat sig vara ett bra alternativ till roterande instrument för avlägsnande av kariös vävnad.

# LIST OF PAPERS

This thesis is based on the following studies, referred to in the text by their Roman numerals.

- I. Almhöjd US, Norén JG, Arvidsson A, Nilsson Å, Lingström P. (2014) Analysis of carious dentine using FTIR and ToF-SIMS. *Oral Health Dental Manag* 13:735-744.
- II. Almhöjd US, Lingström P, Melin L, Nilsson Å, Norén JG. (2015) Staining of carious dentine using dyes with covalent and electrostatic binding properties – an *in-vitro* study. *Oral Health Dental Manag* 14:194-200.
- III. Almhöjd US, Lingström P, Nilsson Å, Norén JG, Siljeström S, Östlund Å, Bernin D. (2017) Molecular insights into covalently stained carious dentine using solid-state NMR and ToF-SIMS. Submitted for publication.
- IV. Lai G, Capi CL, Cocco F, Cagetti MG, Lingström P, Almhöjd U, Campus G. (2015) Comparison of Carisolv system vs traditional rotating instruments for caries removal in the primary dentition: A systematic review and metaanalysis. *Acta Odontol Scand* 73:569–580.

# CONTENTS

ABBREVIATIONS .....	IV
BRIEF DEFINITIONS .....	VI
1 INTRODUCTION .....	1
1.1 Background .....	1
1.1.1 Dental caries .....	1
1.1.2 The caries lesion .....	3
1.2 The sound and carious dentine .....	4
1.2.1 A macroscopic perspective .....	6
1.2.2 A microscopic perspective .....	8
1.3 Detection of the chemical alterations related to the caries progress ...	12
1.4 Chemo-mechanical excavation .....	14
1.5 Choice of methods .....	16
2 AIM .....	19
3 MATERIALS AND METHODS .....	21
3.1 Tooth samples .....	21
3.1.1 Sample denominations .....	21
3.1.2 Sample preparations .....	23
3.2 General analytical methods .....	28
3.2.1 Infrared spectroscopy (FTIR-ATR) .....	28
3.2.2 Mass spectrometry (TOF-SIMS) .....	29
3.2.3 Nuclear magnetic resonance spectroscopy (solid-state) .....	30
3.3 Specific methods .....	32
3.3.1 FTIR (Paper I) .....	32
3.3.2 ToF-SIMS (Papers I and III) .....	33
3.3.3 Light microscopy (Paper II) .....	33
3.3.4 Solid-state NMR (Paper III) .....	34
3.3.5 Light Microscopy .....	34

3.3.6 A systematic review of deciduous dentition using Carisolv or burs (Paper IV).....	35
4 RESULTS.....	37
4.1 Chemical alterations in carious tissue .....	37
4.2 Binding properties with Lucifer yellow .....	40
4.3 Binding properties with hydrazine .....	43
4.4 Visualisation of the covalent binding with hydrazine .....	45
4.5 Visualisation of the covalent binding after chemo-mechanical excavation .....	47
4.6 Systematic review of traditional burs vs. chemo-mechanical caries removal.....	49
5 DISCUSSION .....	51
CONCLUSION.....	63
6 FINAL REMARKS.....	65
ACKNOWLEDGEMENT .....	67
REFERENCES .....	69

# ABBREVIATIONS

AGE	advanced glycation end products, similar to Maillard
D&C	colours approved by the Food and Drug Administration for use in drugs and cosmetics
<sup>13</sup> CNMR	nuclear magnetic resonance spectroscopy of the carbon isotope with the spin quantum no. ½ (natural abundance, 1.1%)
CP	cross polarization
FD&C	colours approved by the Food and Drug Administration for use in food, drugs and cosmetics.
FTIR	fourier transform infrared spectroscopy
FTIR-ATR	fourier transform infrared spectroscopy-attenuated total reflection
ToF-SIMS	time-of-flight secondary ion mass spectrometry
MAS	magic angle spinning
Millie Q	ultra-pure water
<sup>15</sup> NNMR	nuclear magnetic resonance spectroscopy of the nitrogen isotope with the spin quantum no. ½ (natural abundance, 0.4%)
NZ	normal zone of dentine
PG	propylene glycol
PPG	polypropylene glycol
Rf	radio frequency
STZ	sub-transparent zone of carious dentine
TZ	transparent zone of carious dentine



# BRIEF DEFINITIONS

Carious dentine	The affected dentine; soft, discoloured and infected. Contains Maillard- and esters
Dental lesion	A cavity or progression of the carious process from the enamel-dentine junction to the pulp area
Hemiacetal	A reducing sugar with a free hydroxyl group (-OH) on C1
Maillard product	Formed in a reaction between a reducing sugar and the amino group of an amino acid or protein. The final product holds an imine (C=N) function, i.e. a Schiff base
N- (di) acyl	Nitrogen next to an acyl group (N-C=O), as a part of an amide
Sound dentine	The dentine tissue with no signs of infection. Hard and uncoloured. Also called healthy tissue or normal tissue
Sugar acetals	Acetals (or glycosides), sugars with ether linkage (C-OR) formed at the hemiacetal carbon (C1) with the loss of water

# 1 INTRODUCTION

## 1.1 Background

### 1.1.1 Dental caries

The pathological event, i.e. an ecological shift in the diversity and amount of bacteria in the dental biofilm <sup>1</sup> is the origin of one of the world's best-known diseases, namely dental caries. <sup>2</sup>

Even if the ethology of the caries disease is currently well known, it is still a condition affecting the majority of individuals worldwide, even exceeding the prevalence of many medical conditions. <sup>1, 3</sup> A clear reduction in caries prevalence has been seen in the younger age groups during the last few decades, but it is now well known that the disease has a very skewed distribution from both an international and a national perspective. <sup>4, 5</sup> Increasing caries problems have recently also been observed among elderly individuals who retain a large number of their teeth to a high age. The disease is known to be influenced by different biological and socio-economic factors and both medical conditions, as well as global immigration, are examples of factors, which play an important role in this respect.

The biological aspects of and the interaction between the tooth, the microflora and the diet are known as the Keyes triad. <sup>6</sup> When assessing the risk of an individual developing the disease and following the disease progression from a biological perspective, the number and type of microorganisms and the intake of carbohydrates are well-known factors that need to be evaluated. Today, the oral cavity is looked upon as an ecological system where an imbalance between disease-promoting and protective factors determines whether or not the caries disease will develop. <sup>7</sup> The cariogenic potential of the dental biofilm is often assessed by measuring the acidogenic potential, i.e. plaque pH in normal conditions or after sugar exposure. <sup>8</sup>

In all age groups, not least in the younger age groups, a great effort is being made to cope with the factors involved in disease initiation and progression. The most important prevention methods include strategies designed to change the oral environment, i.e. primarily dietary modification, and to strengthen the tooth surface or enhance the potential for remineralisation to the greatest extent by using fluoride. <sup>9</sup> The introduction of fluoridated

toothpaste is regarded as the main reason for the decline in caries prevalence since the middle of the last century.<sup>9, 10</sup>

For a large number of individuals, the disease process is not prevented and it will lead to a continuing demineralisation process, which, when it reaches a certain level, will be diagnosed as a carious lesion. From its initial stage, when it further spreads into the dentine, it will be judged as a manifest lesion, which often needs to be dealt with using operative treatment.

Restorative procedures have been performed for more than 100 years and, for many dentists, the treatment of the symptoms of caries disease still constitutes the main part of their clinical work and the most common reason for a visit to the dentist. Different strategies for this work, including both excavation methods and the materials that are used, have been used over the years. In the early era of operative dental treatment, the principles formulated by GV Black in 1914<sup>11</sup> were the focal point, with the concept of “extension for prevention”. This often resulted in the removal of not only the diseased part of the tooth but also to a large extent healthy tooth tissue. The negative consequences of the excavation principles were often secondary caries and long-term fractures of tooth and filling.<sup>12</sup> Today the general concept of the operative treatment of caries diseases can be summarised in terms of “minimally invasive dentistry”, which focuses on preparation design, excavation techniques and material selection designed only to remove what is absolutely necessary, preserving sound tooth structure and increasing the longevity of the restoration.<sup>13</sup>

The caries-removal part of operative caries treatment can be divided into different parts. It consists of the technical parts, including cavity formation and the excavation process, as well as decision-making in order to establish a caries-free surface. The latter is known to be the subject of great intra- and inter-individual variations. Although known to consist of different zones, during clinical work, carious tissue is often regarded as one homogeneous tissue. Increased knowledge of the exact composition of the carious tissue is considered important in order to increase the potential for more secure restorative work.

## 1.1.2 The caries lesion

The caries disease is a consequence of the interaction between cariogenic microorganisms and dietary carbohydrates. Together with their internal enzymes adding to the tooth surface, the bacteria form a nursing bed for broader colonisation. Bacterial organisms have to attach firmly to the surface in order to avoid being washed away by the salivary flow or by mechanical forces during chewing. Dental caries therefore develops where the microbial deposits are left undisturbed and allowed to accumulate in the biofilm.<sup>6,14</sup>

The symptoms of the disease, i.e. the carious lesion, are the outcome of localised chemical alterations to the tooth surface. These alterations describe the imbalance between the tooth mineral and the fluid in the surrounding biofilm.<sup>1</sup> The shape of the lesion corresponds to the affected area of the biofilm covering the tooth surface that is left to vegetate.<sup>14,15</sup>

A large number of microorganisms, with aciduric and acidogenic properties, play an important role in the initiation and further progression of dental caries.<sup>16-18</sup> The cariogenic bacteria in the dental biofilm extrude organic acids as metabolic by-products that will further affect the hard tissues.<sup>19, 20</sup> If disease progression is not stopped, this may proceed until the tooth is completely destroyed.

The causal factors in the formation of a lesion are the ability of the cariogenic microorganisms to metabolise carbohydrates from the diet<sup>21-24</sup> and to form sugar polymers that will attach to the thin protein layer, i.e. pellicle, on the tooth surface.<sup>15</sup> This causes a reduction in the pH of the dental biofilm<sup>25</sup> caused by extruding organic acids from bacteria harbouring the biofilm.<sup>14, 20</sup> The mineral parts will dissolve in the aciduric environment and this will continue during the supply of organic material to the metabolically active bacteria.<sup>26,27</sup>

The demineralisation process may start when a reduction in plaque pH below pH 5.5, the critical pH of enamel, occurs.<sup>20</sup> The corresponding critical level of dentine is pH 6.2. However, the caries process is inhibited when there is a balance between the calcium phosphate of the enamel and of the saliva. An increase in pH favours the remineralisation of the tooth surface when calcium and phosphate in plaque and saliva can be utilised.<sup>28</sup>

Dental caries is therefore the net result of a complex interaction between matrix bacteria, ingested foodstuffs, saliva components and remnants of

dental mineral, However, as the disease is established, all the factors mentioned above will successively influence the hard tissues, which will lead to the formation of a lesion.

## 1.2 The sound and carious dentine

The tooth consists of enamel, dentine and a pulp compartment. In particular the enamel, but also the dentine, are regarded as non-vital parts, as they are largely composed of inorganic materials, i.e. minerals. The ratios between the inorganic parts, organic parts and water are 95%, 3%, 1% (by weight) for enamel and 70%, 20% and 10% (by weight) for dentine.<sup>19, 29</sup> The pulp constitutes the vital part of the tooth, as it is responsible for vascular transport and subsequently consists of organic matter. However, the dentine is connected to the pulp via the dentinal tubules, which reach into the enamel-dentine junction. The dentine-pulp complex enables linkage via the two tissues where the odontoblast cells and nerve ends can protrude into the dentine.<sup>30</sup>

The enamel is shaped like inorganic rhombohedral crystals with the hydroxyapatite [ $\text{Ca}_{10}(\text{PO}_4)_6(\text{OH})_2$ ] arranged perpendicular to the tooth surface also referred to as biological apatite, due to the fact that the crystal lattice constant can vary as a result of the incorporation of carbonate ( $\text{CO}_3^{2-}$ ) or fluoride ( $\text{F}^-$ ).<sup>31-34</sup> The crystals are largely composed of phosphate groups and calcium ions ( $\text{Ca}^{2+}$ ),<sup>19</sup> which may dissolve when pH falls below the critical levels for enamel and dentine, respectively.<sup>35</sup> The organic content in the enamel consists primarily of enamelin, amelogenin and lipoproteins (about 2% by volume).<sup>33, 36, 37</sup>

The compartment between the tissue cells is called the extracellular matrix. In dentine, the “matrix” is mineralised with hydroxyapatite, which forms the tissue and makes it tough and resilient,<sup>38</sup> because the dentine matrix is less calcified compared with the enamel and contains a larger degree of organic matter, i.e. proteins.<sup>19</sup> Moreover, dentine matrix also contains a network of long fibrous proteins that cross-link with slightly shorter fibrous or globular structures that anchors to the minerals.<sup>39, 40</sup>

More than 90% of the organic matrix in sound dentine represents the scaffold protein collagen predominantly of type I, which forms strong flexible fibres

integrating very tightly to the mineral phase that can be compared to reinforced concrete, in which the building steel represent the fibrous collagen molecule.

The dentinal proteins are often divided into one group of collagens and into one very diverse group of non-collagenous proteins about 10% of the organic matrix <sup>38</sup> (TABLE 1).

The human dentine collagen type I dominate the organic matrix, but also minor amounts of other collagens as III, IV, V, VI have been found <sup>41</sup>. Type III has been detected in patients with dentinogenesis imperfect in reparative dentine of carious dentine and in pulp but never in dentine <sup>42-44</sup>. However, Becker *et al.* suggested type III to be present in dentine and pre-dentine during matrix formation. <sup>41</sup> Nevertheless soluble fragments of collagens of type I, III, VI and XII have been found in non-enzymatically purified protein extracts of carious dentine. <sup>45</sup>

*Table 1. Non-collagenous proteins in dentine*

<i>Non-collagenous proteins</i>	<i>Reports to bind to the mineral</i>
<i>Proteoglycans (PGs)</i> <sup>38, 46</sup>	-
<i>Posphoproteins</i> <sup>44, 46, 47</sup> (PPH, PPL, AG-1)	yes
<i>Gla -proteins</i> <sup>44, 48</sup> (MGPs, Osteocalcin)	yes
<i>Phosphorylated glycoproteins</i> <sup>44, 47</sup>	-
<i>Acidic glycoproteins</i> <sup>44, 46, 49</sup> (Glycoprotein 60, 95 kDa, acidic DSP, Osteonectin)	yes
<i>Serum protins</i> <sup>44</sup> (Albumin, $\alpha$ -2HS glycoprotein)	-

The non-collagenous proteins are mainly acidic in nature and are either phosphorylated or contain a high degree of carbohydrates such as proteoglycans (PG), phosphorproteins (PPH; PPL), Gla-proteins, Ph. Glycoproteins, Acidic glycoproteins and Serum proteins. <sup>38, 44, 46, 47</sup>

The most common non-collagenous proteins in dentine are the phosphoproteins, which are characterised by a high degree of phosphoserines and of varying phosphorylation, highly phosphorylated (PP-H) or low-phosphorylated phosphoprotein (PP-L), respectively. <sup>38, 46</sup> These groups of

proteins are also regarded as the best-known acidic protein, which is a result of the many aspartic acids and phosphate groups.<sup>44, 46</sup> Localised in the mineralised matrix they bind with high affinity to both calcium and hydroxyapatite.<sup>47, 48</sup>

The MGPs (matrix Gla protein) contains Gla-residues and di-sulphide bonding that seemingly binds  $\text{Ca}^{2+}$  more efficiently than other Gla-proteins, in particular,  $\gamma$ -carboxyglutamic acid has been reported to interact directly with the mineral.<sup>44, 49</sup>

Dentine also contains plentiful proteoglycans (PGs) with the dominant side chain composed of glycosaminoglycan (GAGs) mainly of galactose units.<sup>44, 46</sup> One type of PGs, PG II also called Decorine, has been found to bind to collagen type I.<sup>46</sup>

## 1.2.1 A macroscopic perspective

The inorganic crystals are lost (e.g. the enamel and dentine are demineralised) through from the action of carious bacteria. This leaves the organic parts exposed to further reactions. Presumably the only permanent and detectable modification must be within the network of proteins. The organic matrix thus represents the remnants of the demineralisation process when minerals are lost due to the acidic environment.<sup>19, 20, 26</sup> When dentine is demineralised, the phosphoproteins readily dissolve although a minor part is still associated with collagens and forms an insoluble conjugate in the extracellular matrix.<sup>39, 50-52</sup> The other mineral binding proteins, such as the MGPs together with PGs further linked to the collagen molecule, may be released from the minerals, but they will be a part of an insoluble conjugate.<sup>53, 54</sup> In either case the proteins/conjugates might be exposed to further bacterial activity unshielded from the former mineral structure, as a result the progression of a carious lesion will reflect the binding to the demineralisation remnants.

Repeated fluctuations in pH from bacterial acidic attacks in the biofilm lead to a net loss of calcium and phosphate from the mineral and with time this makes the enamel porous. This is seen at the clinic as the first sign of a carious lesion, so-called initial or early caries located in enamel, which can be seen clinically as a white spot lesion or as a dark shadow on the radiograph.<sup>33, 55</sup> As the initial carious lesion continues and intensifies, the

area is increased often leading to an enamel breakdown. Food stain and further acidic producing bacteria give the lesion a darker colour<sup>56</sup>. An early dental carious lesion can be arrested if bacterial plaque is removed, and with an additional contribution of calcium phosphate from the saliva together with fluoride exposure the re-mineralisation of the lesion may occur.<sup>33,34</sup>

During caries progression, tissue breakdown continues and the lesion may finally reach the more vital parts of the tooth such as the dentine and even into the pulp. When the caries process reaches into the dentine, this tissue is softened by microbial acids as the acids dissolves the minerals. This leaves the organic matrix unprotected from enzymatic degradation and further acid exposure. The hydroxyapatite crystals are both smaller in size and less frequent in dentine in comparison to enamel, which presumably increase the dislodging rate of the minerals.<sup>57</sup>

From a clinical perspective the question of how much of the carious tissue that needs to be removed prior to application of a restoration has been discussed. It has been suggested that the outer softer portion needs to be removed before the restoration can be applied while the inner harder part has the capacity to re-mineralize.<sup>58-60</sup>

With the respect to the hardness, using the Knoop hardness test, the carious lesion can be divided into an outer and an inner carious zone from the enamel-dentine junction to the pulp wall. The outer carious layer is discoloured, infected and not possible to be re-mineralised and is Fuchsin-stainable, whereas the inner carious dentine is uninfected and vital and may be remineralised.<sup>58, 61-63</sup> Discolouration has been observed in efforts to distinguish the infected from the non-infected parts in a lesion. However discolouration alone is not regarded as a reliable indicator of an infection,<sup>60, 64</sup> as discolouration is less evident in active caries and bacterial invasion is usually diffuse and extends beyond the discolouration front.<sup>59</sup> This means that the caries process may proceed under the discoloration or not have any discoloration front at all.

In an attempt to combine discoloration, the degree of infection and hardness, it was suggested that the progression stages of a lesion involve the zone of bacterial invasion, the zone of demineralisation, the sclerotic reaction zone and the reactive dentine respectively.<sup>33,63,65</sup> The zone of bacterial penetration also represents the discoloured zone and the outer carious dentine with the lowest Knoop hardness number, whereas the normal dentine zone (NZ) is uncoloured and is the most resilient with respect to the Knoop hardness value. Between these zones is the transparent zone (TZ), described as being

uninfected by bacteria, almost uncoloured and also defined as the inner layer of carious dentine. More recently, a new zone has been described as being present between the transparent zone (TZ) and the normal healthy zone (NZ), the sub-transparent zone (STZ). In contrast with the collagen in the (TZ), the (STZ) is hardly altered and should therefore be reserved for reparative purposes.<sup>66</sup>

Finally in order to accurately excavate the affected zones of the lesion, knowledge of the carious tissues compositions is crucial in developing more secure restorative work.

## 1.2.2 A microscopic perspective

The dental lesion contains bacteria, bacterial cell membranes, enzymes, food remnants and other components from the oral cavity. Consequently, caries is biochemically very complex and non-uniform yet seemed glued together by the more or less degraded organic parts. Microscopic and histological studies on dental caries have revealed a porous, amorphous and fibrous tissue and it has been shown that the main constituents are proteins, but of what nature and in what state is still unclear. Therefore a reliable assumption would be to assume that the bulk of carious tissue consist of interconnecting forces between more or less disrupted collagen cross-linked with other proteins of which many are glycosylated.<sup>38</sup> As a result the organic phase is not disintegrated and dissolved as is the mineral and the remaining bulk of carious tissue is very well anchored to the cavity floor. A lot of scientific works have been performed during the years,<sup>47, 53, 58, 61, 66-70-76</sup> still there is more to be done about the chemical nature of the caries process as well as of the chemical composition and structure of carious tissue.

The organic part of dentine consists of very different classes of proteins (see section, 1.2), but they all hold peptide bonds. (FIGURE 1, in red). The partly restricted bond consists of two different functional groups, the carbonyl (C=O) and the amino group (-NH) respectively.

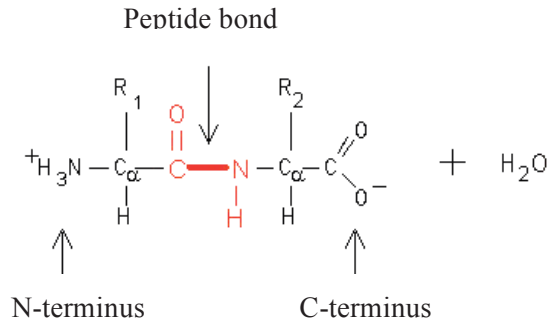


Figure 1. Small peptide with the N-terminus, the C-terminus and the peptide bond in red

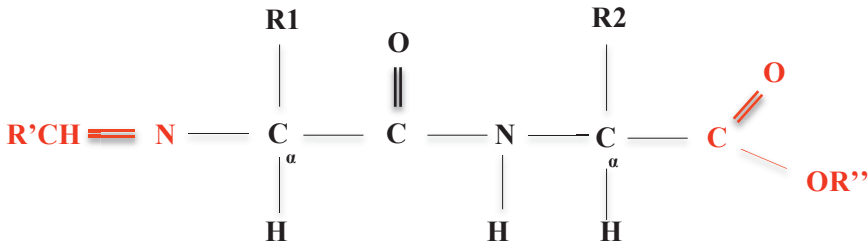


Figure 2. Maillard function on the N-terminus after reaction with carbohydrate and an ester function on the C-terminus after reaction with carbohydrates (or an alcohol function), respectively. R' could be of carbon chain or H.

As a consequence of acidic hydrolysis caused for instance of bacterial acids protonated groups such as carboxylic acid (COOH) or protonated amines ( $\text{NH}_3^+$ ) are formed after hydrolysis of the peptide bond. In addition, carious tissue is reported to be highly protonated<sup>21, 67-68</sup> and may further react with carbohydrates, amino acids, or foodstuff in forming products significant for the carious tissue.<sup>67-68</sup>

Previous studies of dental caries have revealed reactions between proteins i.e. the nitrogen of a free amino end and sugars in producing advanced glycation end products (AGEs; generally called Maillard).<sup>69-70</sup> As seen in (FIGURE 2, N-terminus in red and FIGURE 3). It has also been found that the AGEs are

mainly positioned in the triple-helix region of the collagen molecule and are fairly resistant to the proteolysis activity of pepsin.<sup>77</sup>



Figure 3. *A visible lesion on a caries affected tooth referred to as Maillard reaction products.*

In addition to the Maillard reactions, other organic molecular alterations may occur in the carious tissue. Presumably there are also reactions between the carbonyl function (C=O) of the proteins and carbohydrates as well. (FIGURE 2, C- terminus in red).

It can be hypothesised that the organic acids in the carious tissue catalyse the esterification of the carboxylic acid side chains of the proteins in the presence of carbohydrates or other structures containing alcohol functions in a process similar to the Fischer esterification.<sup>68, 80</sup> The Fischer esterification progress is illustrated in FIGURE 4.

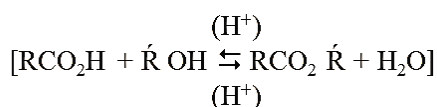


Figure 4. *The formation of an ester by the Fischer esterification reaction. The reaction represents an equilibrium that is catalyzed by acids (low pH) both ways. A large amount of water will direct the reaction towards the formation of carboxylic acids.*

The presence of esters in carious dentine has been investigated and it has been found that esterase's are more common in carious tissue, than in intact

tissue.<sup>78</sup> Moreover, esters deriving from bacterial lipid components such as cholesterol esters have been recognised in both sound and carious dentine.<sup>79</sup> There are also plausible esters formed, when bacteria metabolise substances like sugars and salivary glycoproteins pyruvate are converted to lactate (an ester).<sup>21</sup> Furthermore there is natural occurrence of lactones (cyclic esters) in a caries lesion derived from signal substances among *S. mutans* and *Lactobacilli*, respectively.<sup>81, 82</sup> Esters are more prone to be hydrolysed near the saliva because of the high water content and therefore less frequent in the outermost layer of the lesion. Subsequently they are more likely to be found in the inner layer of carious dentine where the water content is lower.

Different chemical reactions have been used in order to visualise dental caries.<sup>83</sup> Ester can be reacted with one such staining, forming a covalent amid bond with hydrazine derivative.<sup>80</sup> If the hydrazine molecule is part of a chromophore it can be visualised (FIGURE 5, also structure [*d*] in FIGURE 6).

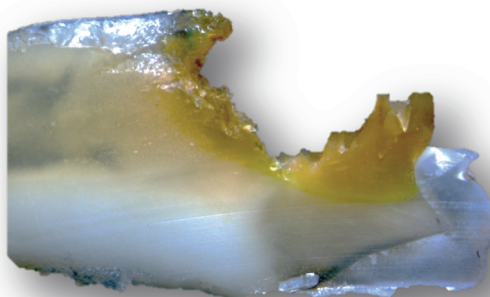


Figure 5. Section of a tooth where hydrazine derivatives (*Amino Fluorescein C536*, *Life technologies*) react with the carious tissue.

Both the Maillard reaction product and the esters are of covalent character, e.g. strong bonds, and may therefore describe one of many strong inter-connecting forces of the carious tissue linked to the proteins in the cavity floor.

### 1.3 Detection of the chemical alterations related to the caries progress

In addition to tactile and visual control, the use of caries detectors has been suggested in order to distinguish carious dentine from sound dentine during the excavation process.<sup>84-88</sup> The reason for this is to help in the decision process prior to sealing the cavity as to whether or not the cavity is caries free. Today, a variety of chemical substances are used for this purpose with active colouring, such as acid red, basic fuchsin, FD&C or D&C in gel formulation respectively. All of them contain electrostatic groups. (TABLE 2)

Table 2. Caries detectors reported from the literature.

<i>Stain/dye in accordance with scientific papers</i>	<i>Manufacturer</i>	<i>Content Dye/gel</i>
<i>Basic fuchsin</i> <sup>83, 89</sup>	-	<i>0.5% Basic fuchsin in PG</i>
<i>Caries Check</i> <sup>TM 88, 90, 93</sup>	<i>Nippon Shika, Japan</i>	<i>1% Acid red or 1% Brilliant blue-FCF in PPG</i>
<i>Caries Check Red</i> <sup>TM 91</sup>	<i>Nishika Co., Yamanashi, Japan</i>	<i>1% Acid red 52 or Brilliant Blue dye in PPG (300 Mw)</i>
<i>Caries Check Blue</i> <sup>TM 91</sup>	<i>Japan</i>	<i>Brilliant Blue dye in PPG (300 Mw)</i>
<i>Caries Detector</i> <sup>TM 58, 85, 90, 92, 93</sup>	<i>Kuraray, Medical Inc, Japan</i>	<i>1% Acid red in PG</i>
<i>Caries Detector</i> <sup>TM 91</sup>	<i>Kuraray America USA</i>	<i>1% Acid red 52 in PG</i>
<i>Caries Finder G</i> <sup>92</sup>	<i>Danville Materials, USA</i>	<i>FD&amp;C green dye in PG</i>
<i>Caries Finder Red</i> <sup>TM 91</sup>	<i>Danville Materials, USA</i>	<i>Acid red 52 in PG</i>
<i>Sable SEEK</i> <sup>TM 92</sup>	<i>Ultradent Products, USA</i>	<i>FD&amp;C green dye in glycol base</i>
<i>SEEK</i> <sup>TM 92</sup>	<i>Ultradent Products, USA</i>	<i>D&amp;C red dye in glycol base</i>
<i>Snoop</i> <sup>TM 92</sup>	<i>Pulpdent Corp., USA</i>	<i>Blue (patented) in PG</i>

Scepticism related to the use of dyes is reported in the literature, as they have been found to be non-selective, with the excessive excavation of sound

dentine as the result.<sup>63, 64, 90, 92, 94-100</sup> Staining with for example Acid Red has shown that the substance may also stain un-altered collagen in sound dentine resulting in over-excavation when all red-stained dentine is removed.<sup>92, 94 97-98</sup>

Demineralised enamel and dentine contain cations ( $\text{Ca}^{2+}$ ) and free protonated amines ( $\text{NH}_3^+$ ) to which negatively charged groups ( $\text{SO}_3^{2-}$ ), such as the substance acid red, could be attracted.<sup>85</sup> Sound dentine also contains charged groups to which dyes with oppositely charged groups can be added,<sup>101</sup> which means that many dyes currently used in clinics may be unspecific (reaction schedules in (FIGURE 6, structure [c]).<sup>90</sup>

It is possible to speculate about whether covalent and specific binding may occur between the hydrazine or a chromophore containing a hydrazine part and specific functional groups in carious dentine. One such chromophore is the substance Lucifer yellow. The only reactive part of the Lucifer yellow system that is able to form a covalent bond with the carious tissue is the hydrazine function that will react with carbonyl structures to form a new peptide or an acyl-substituted hydrazine product.<sup>102</sup> See the reaction models in the reaction scheme in FIGURE 6, structure [d].

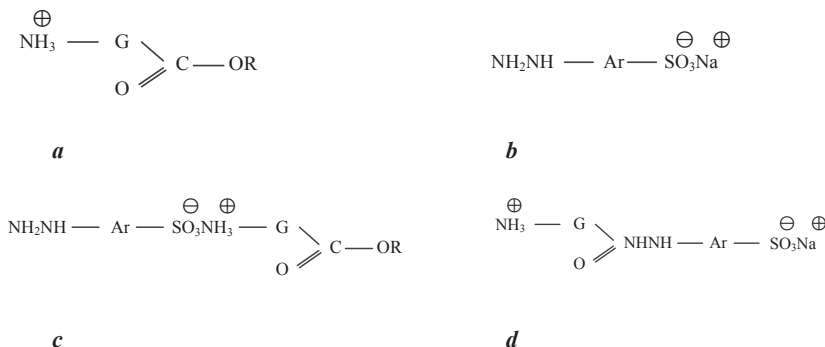


Figure 6. Suggested reactions between carious dentine and hydrazine derivative. Structure [a] shows the caries-specific group (COO-R), structure [b] shows a hydrazine derivative ( $\text{NH}_2\text{NH}_2$ ), structures [c] and [d] represents the reaction products when the hydrazine derivative reacts electrostatically and covalently respectively with the carious tissue.

Structure [a] in FIGURE 6 shows the protonated group ( $\text{NH}_3^+$ ) and the caries-specific group (COO-R) formed in a suggested esterification process after the acid hydrolysis of a dentinal protein. Structure [b] in FIGURE 6 shows a hydrazine derivative with the reactive hydrazine ( $\text{NH}_2\text{NH}_2$ ) and the electrostatic sulphate group ( $\text{SO}_3^-$ ). Structures [c] and [d] in FIGURE 6 represent the reaction products when the hydrazine derivative reacts electrostatically and covalently respectively with the carious tissue. The ammonium ion in [a] has reacted electrostatically with the  $-\text{SO}_3^-$  group and the stain has formed an ion pair, a salt structure [c]. The hydrazine function  $-\text{NHNH}_2$  in structure [b] has reacted with the ester function of structure [a] to form an amide [d] in a covalent binding manner.

## 1.4 Chemo-mechanical excavation

The actual caries excavation process can be performed using different techniques. The most common, both from an historic perspective but also among modern clinicians, is the use of rotating burs. Excavation using this technique is both quick and efficient, but it may be painful for the patient and often requires the use of anaesthesia. Removing carious tissue completely without damaging healthy tissue requires great skill, but it is seldom possible even for an experienced dentist. For deep cavities, the use of rotating instruments is even unsuitable due to the risk of breaking through the inner dentine wall and damaging the pulp. Consequently, alternative carious excavation methods have been developed.<sup>103</sup> They include chemo-mechanical excavation, laser technology and air abrasion. They are all known to differ in the way they affect sound and diseased enamel and dentine and are known to vary in terms of both advantages and disadvantages.

During the last few decades, an alkaline gel system has been introduced onto the market. This chemo-mechanical technique (Carisolv) displays good properties during the excavation of carious dentine, without any negative effects on healthy tooth substance or negative side effects on other oral tissues. Upon application, the two-component caries-disrupting gel softens the carious dentine to an extent where it can then easily be removed with specially designed hand instruments. Apart from successfully removing the carious dentine, this technique has been found to have little or even no effect on mineralised healthy dentine.<sup>104-110</sup> It has also been found to be patient-friendly, with the perception of less pain and an overall increase in comfort

<sup>111</sup> Negative aspects mentioned are the fact that access first has to be reached using other instruments for those lesions not directly accessible and a longer treatment time compared to the use of rotating burs.<sup>112</sup>

The gel consists of a mixture of sodium hypochlorite and different amino acids in a mechanism through which the sodium hypochlorite transfers the chlorine atom to the amine function forming chloramines.<sup>113-117</sup> See FIGURE 7. Earlier investigations report that the dentinal proteins act to start the destruction of the carious tissue.<sup>108, 118</sup>

Furthermore, the chlorination rate is reported to be lower for the reaction with amides in proteins than for the reaction with single amino acids,<sup>117</sup> that is thought to be the reason why it is less susceptible to intact tissue. A larger number of mono-chlorinated amino acids (RNCl) compared with dichlorinated amino acids (RNCl<sub>2</sub>) are formed in the alkaline environment of the sodium hypochlorite gel.<sup>113, 114, 116, 119</sup> the outcome of the chlorination seems to be depended on the pH<sup>113, 119</sup> of the gel. In addition; formations of chloramines are also highly depending on the concentration of the substrates.<sup>113, 114</sup> The chlorinated amino acids in the gel may serve as a reservoir for chlorine to be transferred to the carious tissue,<sup>120</sup> as chlorinated amino groups of the amino acids might transfer chlorine to other amino-containing substrates in the carious tissue (FIGURE 7).<sup>108, 116-117</sup>

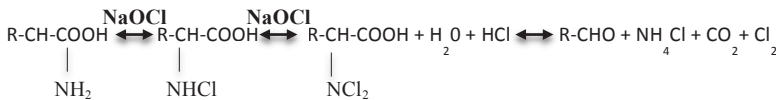


Figure 7. The suggested formation of a chloramine by a two-step oxidation process highly dependent on the pH.

The overall effect of Carisolv mainly involves redox reactions starting with the chlorination of amino groups in the carious tissue. Likewise alcohol functions in the carious tissue may also be affected by the oxidising agent hypochlorite. In all, the oxidation processes takes part in the decomposition of the carious tissue. The decomposition process may involve radicals as well as ionic mechanisms. Thus playing an important roll in removing without drilling.<sup>121</sup> The decomposition of the carious tissue caused by hypochlorite may in part follow modelled illustrated in See FIGURE 7 of the

decomposition of an N- chlorinated amino acid

Cariou dentine is highly glycosylated<sup>67-68</sup> and therefore contains plentiful glucosidic bonds that might be oxidised by sodium hypochlorite solutions.<sup>122</sup> Even so, there is a need for a more detailed investigation of the way these reactions work in concert and of how Carisolv decomposes the carious tissue.

The clinical efficiency as well as advantages and disadvantages of the chemo-mechanical technique using the Carisolv gel have been extensively studied over the years.<sup>123-125</sup> It as early after the technique was introduced found that the treatment time was slightly longer, less need for anaesthesia and that no adverse reactions could be found.<sup>104, 124, 125</sup> However, during the planning of this thesis there were still a limited number of systematic reviews and meta-analyses with focus on this technique found in the literature.<sup>126-128</sup>

Furthermore, combining the chemo mechanical excavation with specific caries stains is not yet fully investigated why there is a need for linking these techniques into a clinically situation.

## 1.5 Choice of methods

In order to avoid the misgivings and complexity associated with the many different purification steps, this thesis focuses on analysing powdered samples of carious dentine with the organic part still attached to the mineral. For this reason, the choice of methods is crucial for these preparations and also for the results.

Extracting intact proteins is a challenging process. The complexity associated with the solubilisation of the mineralised tissue, including both sound dentine and carious dentine, requires both enzymes and acids to be solubilised. Human dentine has been found to be susceptible to trypsin, after which demineralisation by acids can occur.<sup>129</sup> However, it has been found that proteins can also be extracted without enzymes under mildly acidic conditions with additional sonication, although this is a time-consuming technique with many uncertainties in the numerous purification steps that are involved.<sup>45</sup>

Over the years, a variety of techniques have been used in order to identify chemical alterations in carious tissue. They range from separation techniques, to surface chemistry analysis and histological analysis.

The solubilisation of the carious tissue enables liquid analytical separations. One of them is the Positive Elson-Morgan reaction (a colorimetric determination), where amino sugars that are formed can be separated according to their charges by liquid chromatography. This is taken as evidence of the presence of carbohydrates in carious dentine.<sup>68, 71</sup> Non-enzymatic crosslinks formed between sugar and protein from collagen digests of carious dentine tissue reactions such as pentosidine have been analysed by fluorescence measurements.<sup>69-70</sup> The fragmentation of collagen in carious dentine has been found after separation by sodium dodecyl sulphate (SDS) gels, followed by mass spectrometric analysis.<sup>45</sup>

Chemical alterations in hard tissue after different treatments, such as using rotary instruments, with chemo-mechanical techniques, after etching and adhesives to dentine and carious tissue have been frequently analysed with Fourier Transform Infrared Spectrum (FTIR) and scanning electron microscopy (SEM).<sup>26, 66, 72</sup> These methods do not require extensive sample preparation and protein purification prior to the analysis.

ToF-SIMS is a more modern method and may add important information after different treatments of dentine and/or carious dentine in the solid state. It has been found that chemical changes in carious dentine can be detected using this technique.<sup>53, 132</sup>

Dentine surface analysis after different excavation techniques has previously been deduced by atomic force microscopy (AFM) and scanning electron microscopy (SEM).<sup>107, 109</sup>

Surface dentine after chemo-mechanical treatment has been found to be unaffected, with no remnants from the added chemicals observed and no alterations in the mineral phase of the dentine composition. Furthermore, micro-CT (X-ray) analyses have been used for the establishment of the caries-free surface in determining the caries removal effectiveness (CRE).<sup>90</sup>

Nuclear magnetic resonance, such as <sup>13</sup>C NMR and <sup>15</sup>N NMR, has recently been used to observe binding between dentine and dental adhesive. However a more recent technique, solid-state NMR, has been used for studies of structural changes in whole or sectioned teeth.<sup>131, 133</sup>

Histological analysis of the collagen distribution of bacteria has been evaluated using light microscopy with the aid of dyes.<sup>58, 61, 83, 94</sup> However, often an unwanted staining of non-cariou dentine might occur.<sup>92, 97</sup> The opportunity to analyse the colour changes of longitudinally sectioned lesions without adding any dye, using reflective light photomicrography, has been reported.<sup>135</sup> However, stereomicroscopy tends to over-score the lesion and, as a result, the addition of dye is still regarded as more accurate and reliable.<sup>86</sup> Consequently, stereomicroscopic analysis with digital photographs on sectioned lesions can be regarded as useful for the detection of dyes in dental hard tissues.

An attempt was therefore made to find unique groups (chemical alterations) incariou dentine, hopefully not found in dentine by FTIR and Tof-SIMS. Another challenge was to confirm the existence of these unique groups (presumably esters) by covalent bonding with hydrazine and therefore considered for light-microscopic analysis and NMR. The hypothesis was that there were unique groups found in cariou dentine not detected in sound dentine, that these groups will react with hydrazine derivate and that the type of binding of different dyes to cariou dentine varies. Finally, although chemo-mechanical removal of dental caries using Carisolv have been used clinically since the mid of 1990's, there is limited evaluation when used in the primary dentition. Thus, the second hypothesis of this thesis was that the of this technique, when systematically evaluated, corresponds to what is seen for.

## 2 AIM

The overall aim of present study was to confirm if there are any stable chemical alterations in carious dentine in comparison to sound dentine. To be able to distinguish these parts or groups from un-affected parts of the mineralised tissue, tissues were stained with specific dyes “carrying a hydrazine group”. The marked carious tissue can then be excavated preferably using the chemo-mechanical technique.

In more detail, the specific aims were:

- to identify unique chemical alterations, i.e. ester function groups, in outer and inner carious dentine not found in sound dentine.
- to verify the presence of the ester groups by reacting with hydrazine derivative.
- to elucidate the type of binding capacity (electrostatic or covalent bond) of different dyes to carious dentine.
- to confirm the covalent bonding between a hydrazine based isotope and the carbonyl functions of carious dentine.
- to systematically evaluate the clinical relevance of the chemo-mechanical system specified for excavation of carious dentine in the primary dentition.



## **3 MATERIALS AND METHODS**

### **3.1 Tooth samples**

#### **Papers I-III**

For Papers I-III, permanent teeth with dentinal caries that had been extracted were collected from the local emergency dental clinic in the city of Gothenburg. The teeth were donated by the patients of their own free will for experimental purposes after they had been given information about the study. All the teeth had open carious lesions and so the carious dentine was accessible without any drilling. As reference teeth for sound dentine, premolars extracted prior to orthodontic treatment at the Department of Paediatric Dentistry, University of Gothenburg, were used. Both the children and their parents were informed about the aim of the study and had given their verbal consent. After extraction, all the teeth were handled without any identification, so that none of the teeth could be traced back to any specific individual. The teeth were stored in separate plastic tubes under humid conditions (1% NaCl, +4°C) until analysed.

#### **3.1.1 Sample denominations**

#### **Papers I-III**

Various preparations and analytical methods for sound dentine and carious dentine were used in the different papers (I, II and III), shown in TABLE 3.

Table 3. An overview of the sample ID and analytical methods in the different studies

Paper no: /sample	Tissue/treatment	Analytical method
I: S01-SD	Sound dentine <sup>1</sup>	FTIR (KBr)
I: S02-SD	Sound dentine	FTIR (KBr)
I: S03-ICL	Caries – inner <sup>2</sup>	FTIR (KBr)
I: S04-ICL	Caries – inner	FTIR (KBr)
I: S05-OCL	Caries – outer	FTIR (KBr)
I: S06-OCL	Caries – outer	FTIR (KBr)
I: S07	Sound dentine, untreated (reference)	FTIR-ATR
I: S08	Sound dentine, Lucifer yellow/NaOH <sup>3</sup>	FTIR-ATR
I: S09	Sound dentine, NaBH <sub>4</sub> /Lucifer yellow/ethanol	FTIR-ATR
I: S10	Caries – inner, untreated (reference)	FTIR-ATR
I: S11	Caries – inner, Lucifer yellow/NaOH	FTIR-ATR
I: S12	Caries – inner, NaBH <sub>4</sub> /Lucifer yellow/ethanol	FTIR-ATR
I: S13	Caries – inner, untreated (reference)	FTIR-ATR-ToF-SIMS
I: S14	Sound dentine, untreated (reference)	FTIR-ATR ToF SIMS
I: S15	Caries– inner, Lucifer yellow/NaOH	FTIR-ATR-ToF-SIMS
I: S16	Sound dentine, Lucifer yellow/NaOH	FTIR-ATR-ToF-SIMS
II: FB	Carious dentine, Patent Blue, NaCl/NaOH <sup>2</sup>	Microscope
II: AR	Carious dentine, Acid Red, NaCl/NaOH	Microscope
II: AF594	Carious dentine, AlexaFluor594 hydraz,NaCl/NaOH	Microscope
II: AFS	Carious dentine, Aminofluorescein, NaCl/NaOH	Microscope
II: LYCH	Carious dentine, Lucifer yellow.NaCl/NaOH	Microscope
II: FB+CH	Carious dentine, PatentBlue+Lucifer y NaCl/NaOH	Microscope
II: FB+AS	Carious dentine, PatentBlue+Aminoflu.NaCl/NaOH	Microscope
III: ND	Normal dentine, reference <sup>1</sup>	ToF-SIMS-NMR
III: CD	Carious dentine, reference <sup>2</sup>	ToF-SIMS-NMR
III: NDH1	Normal dentine, <sup>15</sup> N <sub>2</sub> -hydrazine/water (HY) wash1 <sup>3</sup>	ToF-SIMS-NMR
III: NDH2	Normal dentine, <sup>15</sup> N <sub>2</sub> -hydrazine/water (HY) wash-2	ToF-SIMS-NMR
III: CDHY1	Carious dentine, <sup>15</sup> N <sub>2</sub> -hydrazine/water (HY) wash-1	ToF-SIMS-NMR
III: CDHY2	Carious dentine, <sup>15</sup> N <sub>2</sub> -hydrazine/water (HY) wash-2	ToF-SIMS-NMR
III: CDHY	Carious dentine, <sup>15</sup> N <sub>2</sub> -hydrazine/water (LYHY)	ToF-SIMS-NMR

<sup>1</sup> Published data on unaffected dentine designated sound dentine in Paper I and normal dentine in Paper III. They still represent the same type of tissue.

<sup>2</sup> Carious inner layer Paper I is of the same kind as carious dentine in Paper III. For Paper II, carious dentine represents the whole affected area of the tooth sections.

<sup>3</sup> Lucifer yellow (=hydrazine derivative HD) in Paper I, whereas hydrazine derivative in Paper II represents three different dyes and, in Paper III, hydrazine HY (= <sup>15</sup>N<sub>2</sub>H<sub>4</sub>) is not a derivative.

## 3.1.2 Sample preparations

### Paper I

Paper 1 was performed as three different substudies, *Parts I-III*. An overview of the experimental design is given in FIGURE 8. A total of 15 permanent molars were used for 16 different samples. The collection of sound and carious dentine was carried out by an experienced clinician using a hand excavator and by drilling under a normal dental operation light using magnification glasses. After removing the outermost parts of the carious tissue with a hand excavator, two layers (inner and outer) of the carious dentine were identified.<sup>62</sup> After excavation to hard dentine of normal colour, tested using a tactile procedure,<sup>136</sup> sound dentine was collected from the same tooth using rotating burs. Tissue from the two layers of carious and sound dentine were collected, rinsed in purified water and stored separately in Eppendorf tubes, which were left to dry in an ambient temperature.

Sixteen pulverised samples **S01-S16** were obtained for FTIR-ATR and ToF SIMS analyses denoted as *Part I S01-02-SD; S03-04-ICL; S05-06-OCL. Part II S07-S12 and Part III S13- S16*. (TABLE 3 and FIGURE 8). The pulverised samples in *Part I* were mixed with potassium bromide (KBr) and the mixture was pressed together into pellets of 100 mg for each sample with no further treatments before subsequent FTIR analysis. In *Part II and Part III*, the powdered sound and carious dentine samples were stained during different time periods with an aqueous solution of a 13 mM hydrazine derivative (Lucifer yellow CH, Sigma). Lucifer yellow is supposed to react with the ester function group discovered in the FTIR analysis in *Part I*. In order to avoid unwanted hydrogen bonding, carious tissue was repeatedly washed with both salt (NaCl, 1 M) and alkaline solutions (NaOH, 0.5 M), **S08, S11, S15** and **S16**, (TABLE 3). In order to prevent reactions between Lucifer yellow and possible aldehydes and ketones that were present, the samples were also treated with the reducing agent, NaBH<sub>4</sub>, in an ethanol prior to the staining, leaving only ester functions for reaction with Lucifer yellow. This means that aldehydes and ketones turn into alcohol functions instead. After subsequently washing with 99% ethanol, samples **S09** and **S12** were treated with a 13 mM aqueous solution of the hydrazine derivative (Lucifer yellow CH, Sigma, USA) (TABLE 3).

For the FTIR-ATR analyses, the pulverised samples were pressed between diamond plates before the analyses. For the ToF-SIMS analyses, the pulverised samples were applied to double-sided conductive tape and mounted on a sample holder for the instrument.

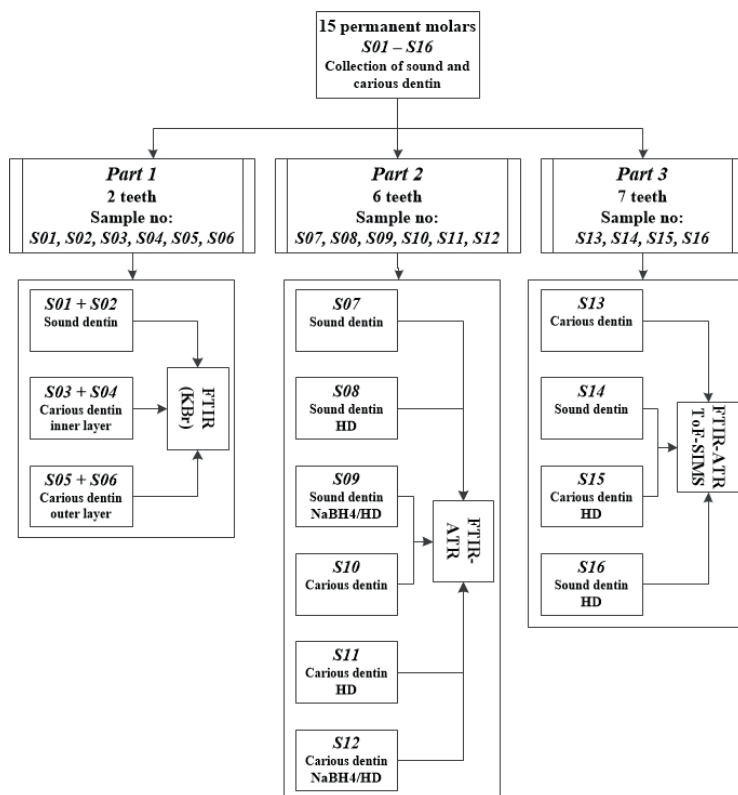


Figure 8. A flow chart of the experimental design in Paper I, Parts I-III.

## Paper II

Four permanent teeth were used for the experiments in Paper II. The teeth were mounted with cold-curing acrylate on holders for the Leica SP1600 Low Speed Microtome (Leica Mikrosysteme Vertrieb GmbH, Wetzlar,

Germany). From each tooth, five sagittal non-decalcified sections with a thickness of 300  $\mu\text{m}$  were cut in the bucco-lingual direction. After cutting, digital images were taken of all sections using a Leica M80 Stereo Microscope equipped with a Leica digital camera. The following five dyes (presented in TABLE 2) dissolved in water were used for the staining experiments: Food blue (FB) Acid red (AR), Alexa fluor 594 (AF594), Amino fluorescein (AFS) and Lucifer yellow CH (LYCH). Two mixed solutions, food blue+lucifer yellow CH and food blue+aminofluorescein, were also used (in all, seven dye solutions). The concentrations were set at 15 mM under a neutral pH for all dyes. In order to evaluate the binding properties of the dyes to carious dentine, the tooth sections were exposed to the different dye solutions for 24 hours, followed by 24 hours in a salt solution, (NaCl, 1M), after which they were exposed to an alkaline solution, (NaOH, 0.5M), for 24 hours. The specimens were thoroughly rinsed with deionised water between the different exposure procedures. For each dye, two sections from two different teeth were used. Before exposure to the dyes, images of the sections were taken. Each section was then placed in a small plastic cup, a drop of the dye (10  $\mu\text{l}$ ) was applied to the carious dentine in the section and the cups were sealed with a lid to prevent them drying out. The experimental design is shown in FIGURE 9.

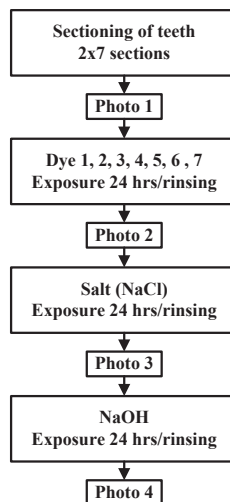


Figure 9. A flow chart over the experimental procedure in Paper II.

### Paper III

Carious dentine was collected from 15 teeth using a low-speed dental bur. After the outermost soft carious dentine had been removed by hand excavation, carious dentine was collected using a low-speed dental bur. Normal sound dentine was obtained from two caries-free premolars using a low-speed dental bur after removal of the enamel with a high-speed dental bur under water cooling. Prior to the staining experiments, the dentine samples were washed and then ground into a dry powder under liquid nitrogen. A total of 68.5 mg of carious dentine (divided into three lots) and 41.5 mg of normal dentine (divided into two lots) were obtained. (FIGURE 10). The stains preparation were prepared and denoted **HY**, **LY** and **HY•LY** (stain preparation can be viewed in Paper III. Material and methods). A flow chart of the dentine samples, staining procedures and analytical methods used is presented in (FIGURE 10). Aliquots of 100 µl from the hydrazine solution **HY** were added to 20.5 mg of carious dentine **CD** and 20.5 mg of normal dentine **ND**. After 24 hours, the samples were washed extensively with ethanol (96%), sodium hydroxide (0.5M) and Millie Q water. The washing procedure was repeated three times. The washed samples were denoted **CD-HY-1** and **ND-HY-1** respectively and analysed with ToF-SIMS spectrometry and NMR spectroscopy. After the analyses, the two samples, **CD-HY-1** and **ND-HY-1**, were washed once more in accordance with the aforementioned washing protocol. The washed samples were denoted **CD-HY-2** and **ND-HY-2** respectively and analysed a second time with ToF-SIMS and NMR. The powdered <sup>15</sup>N<sub>2</sub>-hydrazine-labelled lucifer yellow **HY•LY** was dissolved in Millie Q water (22 ml) and added to 20.5 mg of carious dentine and the mixture was kept at room temperature for 24 hours. In order to remove excessive stain, the sample was washed with slightly alkaline water, followed by washing with Millie Q water through a microfilter funnel. The washing continued until no yellow colour could be detected in the residual water using a UV/VIS spectrometer (Lambda 40 UV/VIS Spectrometer, Perkin Elmer Instruments, USA). The sample was allowed to dry at room temperature (denoted **CD-HY•LY**) and analysed with ToF-SIMS and NMR. (FIGURE 10).

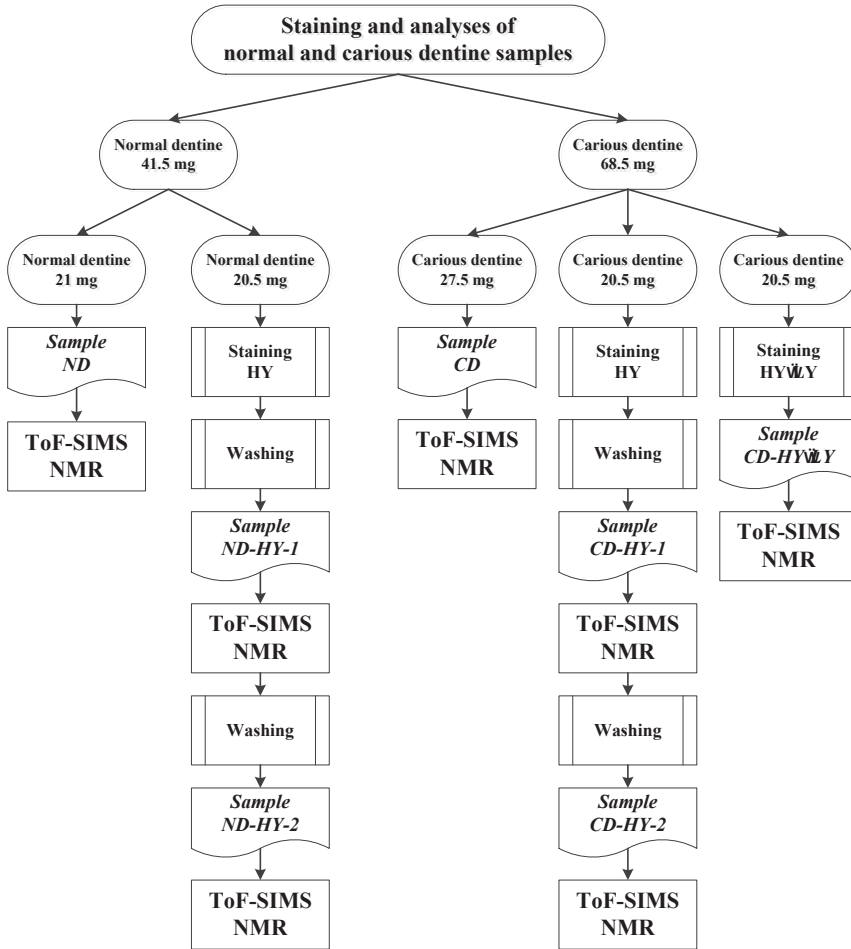


Figure 10. Flow chart showing the experimental procedures of staining and analyses of normal and carious dentine (ND=normal dentine; CD=carious dentine; HY=hydrazine; HY•LY=hydrazine-labelled lucifer yellow; washing=washing according to protocol in the text; ToF-SIMS=Time-of-Flight Secondary Ion Mass Spectrometry; NMR=Nuclear Magnetic Resonance spectroscopy).

## 3.2 General analytical methods

### 3.2.1 Infrared spectroscopy (FTIR-ATR)

Infrared is the light radiation between the visible light and the microwave regions. The frequency region of 400-4,000  $\text{cm}^{-1}$  is of particular interest. Infrared radiation is absorbed and transferred by organic and inorganic molecules into energy of molecular vibrations, rotations and translations. Consequently, the vibrational energy levels of sample molecules transfer from ground state to excited state. The frequency of the absorption peak is determined by the vibrational energy gap between these states and the absorption pattern appears as bands in spectra. The frequency or wavelength of absorptions depends on the relative masses of the atom, the force constant of the bond geometry of the atoms and as a whole the dipole moment of the molecule. The unit is  $\text{cm}^{-1}$  or  $\lambda$ .<sup>137</sup> Charts of the characteristic absorption of infrared radiation of known functional groups are used to determine sample structure, as certain functional groups give bands at the same frequency.

In general, a FTIR spectrometer consists of a source, interferometer, sample holder, detector, amplifier, converter and a computer. In simple terms, the source radiation ( $\lambda$ , micrometer) passes the sample through the interferometer before it reaches the detector.<sup>137</sup> The signal is then amplified and converted to a computer in which Fourier transformation is performed. In addition, the scanning time of all frequencies is short, approximately 1 s, and the resolution is high, 0.1 ~ 0.005  $\text{cm}^{-1}$ . Moreover, the scanning range and accuracy of the wave number are high, ranging from ~ 5,000 - 10  $\text{cm}^{-1}$  and with errors of  $\pm 0.01 \text{ cm}^{-1}$  respectively. Attenuated total reflection (ATR) is used for spectra of solids, regardless of the thickness. It enhances the signal in the IR region by an internally reflected IR beam generated from a dense crystal with a high refractive index in close contact with the sample. This means that the beam of light reflected from the crystal (or a transmitting medium) passes a short distance back from the sample to the crystal. If the sample has lower refractive values than the transmitting medium (crystal), the light passes through the material to a depth of a few micrometres giving an absorption spectrum. The advantages of the ATR technique are minimal sample preparation and the possible analysis of samples in their natural state, less purification, pressing into pellets, grinding and so on.

### 3.2.2 Mass spectrometry (TOF-SIMS)

A mass spectrometer is an analytical tool for molecule identification where a sample is ionised by irradiation from a high-energy source, such as electrons (electro spray (ESI), laser (Matrix Assisted Laser Desorption/ionisation spectrometry, MALDI) or ions, as in secondary ion mass spectrometry (SIMS).<sup>137-140</sup>

TOF devices equipped with the SIMS technique ionise the solid surfaces of the sample by letting high-energy primary ions (ion gun) collide with the sample surface, thereby forming a beam of secondary ions, neutral particles and electrons, subsequently emitting from the surface. ToF-SIMS is also referred to as “static” SIMS, because a low primary ion current is used to “tickle” the sample surface to liberate ions. The secondary ions that form, also called sputtered ions (analyte ion), are then accelerated by an electric field (extraction field), ideally to reach the same kinetic energy ( $\frac{1}{2}m \times v^2$ ;  $m$  is the mass and  $v$  the velocity) and passed into the time of flight mass analyser (TOF) under high vacuum. The ions “fly” through a flight tube to a reflector that focuses them on a detector. A ToF-SIMS spectrum is captured from the exact time (i.e. time of flight) at which each secondary ion reaches the detector relative to the initial primary ion pulse. As the ions have the same kinetic energy but different masses, the lightest ions travel more quickly than the heavier ions and reach the detector first. At the detector, the instrument software is able to convert the raw spectrum (ion counts as a function of arrival time), since the travel time, the flight tube length and the acceleration voltage are known, into a mass spectrum (a function of mass-to-charge ratio  $m/z$ ). In the mass spectrum, the intensity is plotted versus the  $m/z$  (mass-to-charge ratio). Because it is possible to measure the “time of flight” of ions on a scale of nano-seconds, it is possible to produce a mass resolution as fine as 0.001 atomic mass units. It is worth noting that ToF-SIMS only detects the secondary ions that are emitted from the surface (~1% of the emitted particles). Multiple charges are rare, normally the secondary ions of single charges, but a variation in the initial energy will lead to a variation in the time of arrival at the detector. This will reflect the resulting mass spectra of the secondary ions. For this reason, SIMS has appropriate electrostatic fields inserted into the flight part. Ions with larger initial energy will therefore penetrate this field a little further. As a result they have a longer flight part, take longer to arrive at the detector and do so at the same time as their sister ions. SIMS provides more efficient ionisation and reduces the

time of arrival for successively formed molecular ions compared with older ionisation methods<sup>141-142</sup>

### 3.2.3 Nuclear magnetic resonance spectroscopy (solid-state)

Nuclear magnetic resonance (NMR) is the complete analysis and interpretation technique for determining the structure of organic compounds. The NMR spectrometer consists of a magnet, a radio frequency transmitter, which generates a resonance frequency, and a receiver to detect the resonance signals. Resonance relates to the phenomena of transitions that can only occur if the transmitter frequency ( $\nu_1$ ) matches the Larmor frequency ( $\nu_L$ ) of the nuclei studied in the applied magnetic field. Any nuclei that have a spin angular quantum number ( $I$ ) other than 0 can be detected by NMR analysis. For example, the isotopes of hydrogen  $^1\text{H}$  and carbon  $^{13}\text{C}$  have a spin of  $I = \frac{1}{2}$  and are therefore detectable.<sup>143</sup>

In the presence of a static magnetic field ( $B_0$ ) for nuclei with a spin of ( $I = \frac{1}{2}$ ), two possible magnetic quantum numbers ( $m$ ) exist, i.e. the spin states of ( $m=+1/2$ ) and ( $m=-1/2$ ) respectively. The different spin energy states (energy levels) are caused by the behaviour of the nuclei in a magnetic field ( $B_0$ ). A spinning charge like an atomic nucleus generates a magnetic field around itself, resulting in a “spin magnet” with a magnetic moment ( $\mu$ ) proportional to the spin ( $I$ ). As a result, the difference in energy ( $\Delta E$ ) between the two spin states is dependent on the external magnetic field strength ( $B_0$ ). Furthermore, two spin states will have the same energy when the external field is zero, but they diverge as the field increases. The transition energy needed, i.e. ( $\Delta E$ ), to obtain NMR spectra comes from the irradiation of the sample with radio frequency ( $Rf$  or  $\nu_1$ ), where energy corresponding exactly to the spin state separation (matches the Larmor frequency) of a specific nucleus will cause the excitation of those nuclei in the  $+1/2$  state to the higher  $-1/2$  spin state. A transition can only take place between adjacent energy levels.<sup>143</sup>

A transition from a lower to an upper energy level corresponds to absorption, whereas the higher to the lower energy level corresponds to the emission of the electromagnetic waves of appropriate frequency. Either way, both transitions are responsible for the reversal of the spin orientations of nuclei. However, the populations in the lower levels of nuclei are more abundant,

which explains why the absorption of energy is the more dominant process. The signal shown in a spectrum thus equals the absorption process. After the pulse has been withdrawn, the spin system reverts to its equilibrium state by relaxation. The resulting frequency spectrum obtained after Fourier transformation is a result of the difference between the generator frequency and the resonance frequency ( $\Delta E$ ) of the sample. ( $\Delta E$ ) is usually given as a frequency in units of MHz ( $10^6$  Hz).<sup>143</sup>

Commonly, the transition is induced to the sample by a pulse NMR method, as it allows all the nuclei of one species (for example,  $^{13}\text{C}$ ) to be excited simultaneously by a fixed radiofrequency pulse at different time intervals, with the idea that all the nuclei will be irradiated equally in one experiment.

In NMR spectroscopy, there is no absolute spectral scale, as the resonance frequency and the magnetic field are interdependent of one another in the resonance condition. So, as electrons are charged particles, they move in response to the external magnetic field ( $B_0$ ) so as to generate a secondary field that opposes the much stronger applied field. This secondary field shields the nucleus from the applied field, so  $B_0$  must be increased in order to achieve resonance. A relative scale must therefore be used, where one determines the frequency difference between the resonance signal of the sample and that of a reference compound. Historically, the reference compound was added to the sample before each measurement and denominated the internal standard that will also have the chemical shift  $\delta = 0$  from where the shifts are calculated.<sup>143</sup> Today, reference is instead made to the absolute frequency of the spectrophotometer magnet to calculate the shift. For solid-state NMR, an isotropic chemical shift could be revealed under fast magic angle spinning, where the directionally dependent character of the chemical shield is removed.<sup>144</sup>

Samples analysed by NMR can be liquids or solids. Molecular motions are restricted in solids and this results in slow relaxation and chemical shift anisotropy, which causes the line broadening of the solid-state NMR signals.<sup>144-145</sup> A technique that can reduce or remove anisotropy (interactions between nuclei) is sample rotation, which is most frequently performed by magic angle spinning (MAS). In conjunction with cross-polarisation (CP), defined as CP-MAS, this provides much sharper signals than the direct excitation of heterogenic samples (such as powder samples). Using cross-polarisation, the abundant nucleus is excited and its energy is transferred to the observed nucleus. The RF power ratio (the pulses) applied has to be optimised for optimal magnetisation transfer. For example, the polarisation transfer from an  $^1\text{H}$  to a  $^{13}\text{C}$  of the rotating frame must be weaker for the proton channel than

for the carbon channel. CP-MAS is a fundamental element of most pulse sequences in solid-state NMR spectroscopy.<sup>144, 145</sup> It engages the direct excitation of  $^1\text{H}$  spin, followed by CP transfer to another nuclei, and provides improved signal detection for  $^{13}\text{C}$ ,  $^{15}\text{N}$  or similar nuclei.

### 3.3 Specific methods

#### 3.3.1 FTIR (Paper I)

In Paper I, the FTIR-KBR technique was used to analyse the difference in chemical composition between sound dentine and the outer and inner layer of carious dentine. The FTIR-KBr analyses were performed using a Mattson Cygnus 100 FTIR spectrophotometer with  $4\text{ cm}^{-1}$  resolution (Thermo Fischer Scientific Inc., USA). The instrument was purged with analytical instrument quality air to remove atmospheric  $\text{CO}_2$  and  $\text{H}_2\text{O}$  and dried and purified with a Balston type 75-60 air purification system. The spectra were baseline corrected using Omnic FT-IR software (Thermo Nicolet Corp., Madison, WI, USA). For all spectra, the same wave-number positions were chosen. Each spectrum was acquired from 100 scans and the resolution was  $4\text{ cm}^{-1}$ . To enhance and further survey peaks or specific shoulders, a Fourier Self-Deconvolution technique was used, followed by spectral subtraction with sound dentine set as the reference, using the software for the FTIR instrument. The pulverised samples were mixed with potassium bromide (KBr) prior to subsequent FTIR analyses and pellets with a weight of 100 mg were made.

In addition, IR measurements using FTIR-ATR were made to analyse the difference in chemical composition and, more precisely, to investigate the reaction with the possible ester carbonyl function group in carious dentine with hydrazine derivative that would give a change in the IR spectra. The FTIR-ATR analyses were performed using a Nicolet 6700 FTIR spectrophotometer (Thermo Nicolet Corp., Madison, WI, USA). A Smart Orbit diamond micro-ATR attachment was used directly to acquire spectra from the samples. The instrument was purged with analytical instrument quality air to remove atmospheric  $\text{CO}_2$  and  $\text{H}_2\text{O}$  and dried and purified with a Balston type 75-60 conditioner. The dry weight of each sample was approximately 1 mg. Before the analyses, samples representing sound and outer and inner carious dentine respectively were pooled FIGURE 8. For the

FTIR-ATR analyses, the pulverised samples were pressed between diamond plates before the analyses.

### 3.3.2 ToF-SIMS (Papers I and III)

The powdered samples were mounted using tweezers on double-sticky tape on steel blocks in a laminar flow hood. The analysis of the samples was performed in a ToF-SIMS IV instrument (ION-TOF GmbH, Germany) by rastering a 25 keV  $\text{Bi}_3^+$  beam over an area of  $\sim 150 \times 150 \mu\text{m}$  or  $200 \times 200 \mu\text{m}^2$  for 150-200 seconds respectively. The analyses were performed in positive and negative mode at high mass resolution (bunched mode:  $m/\Delta m \geq 4000$  at  $m/z$  30,  $\Delta l \sim 5 \mu\text{m}$ ) with a pulsed current of 0.12 pA.

In Paper I, ToF-SIMS was used to analyse the treatment of sound and carious dentine with a hydrazine derivative (Lucifer Yellow CH, Sigma, Mr: 521 g/mol) in both positive and negative mode. The powdered samples were applied to double-sided tape on a silicon wafer and mounted in the sample holder before analysis. In Paper III, the  $^{15}\text{N}_2$ -hydrazine was used in this study as a simple molecular model of Lucifer yellow. According to their mass-to-charge ratio ( $m/z$ ), the binding effects of  $^{15}\text{N}_2$ -hydrazine and  $^{15}\text{N}_2$ -hydrazine-labelled Lucifer yellow to carious and normal dentine, the intensity (counts) in the positive spectra was observed. The measurements were normalised to the total ion counts, in order to minimise differences in measurement parameters and, as a result, all values were considered to be relative values. The mean values and standard deviations of the intensity of the selected peaks were calculated for each sample.

### 3.3.3 Light microscopy (Paper II)

In Paper II, microscopic analyses of sectioned teeth exposed to different staining methods were analysed. Digital images were taken of the specimens in Study 2 in a Leica M80 Stereo Microscope (Leica M80 with 8:1 zoom,  $\times 0.75$ , Leica Mikrosysteme Vertrieb GmbH, Wetzlar, Germany) in incident light against a matt black background. Digital images were taken of all sections using a Leica digital camera (Leica DFC420 C, Leica Mikrosysteme

Vertrieb GmbH, Wetzlar, Germany) equipped with Leica Application Suite LAS V3.7.0 (Leica Microsystems AG, Heerbrugg, Switzerland).

### 3.3.4 Solid-state NMR (Paper III)

In paper III, the solid-state  $^{15}\text{N}$  and  $^{13}\text{C}$  NMR magic angle spinning (MAS) nuclear magnetic resonance (NMR) experiments were performed on a 14.1 T Agilent Inova spectrometer (Larmor frequency of 60.8 and -150.9 MHz respectively), equipped with a 3.2 mm double-resonance MAS probe.  $^{15}\text{N}$  NMR spectra were obtained using cross-polarisation (CP) with a contact time ranging from 1 to 7 milliseconds and a repetition delay of 2 s at MAS rates ranging from 5 to 14 kHz. The  $^{15}\text{N}$  chemical shift ( $\delta$ ) scale in ppm was calibrated on solid  $^{15}\text{NH}_4\text{Cl}$ , which was set to 39.3 ppm.<sup>154</sup> The second ppm scale, referenced to liquid  $\text{CH}_3\text{NO}_2$ , was computed according to  $\delta(\text{CH}_3\text{NO}_2 \text{ liquid}) = \delta(^{15}\text{NH}_4\text{Cl} \text{ solid}) - 341.168 \text{ ppm}$ . The  $^{13}\text{C}$  CP experiments were performed at a MAS rate of 14 kHz, a repetition delay of 15 seconds and a contact time of one millisecond. The cycloalkane Adamantane was used as a reference for the  $^{13}\text{C}$  chemical shift scale. The spectral width was chosen to observe at least one spinning sideband, if any. The spinal decoupling strength was set to 85 kHz. A moderate non-shifted Gaussian window function of 15 Hz was applied prior to Fourier transformation of the recorded time-domain signal.

### 3.3.5 Light Microscopy

From yet unpublished data (IADR, Florens)<sup>146</sup> the staining of carious dentine from open cavities in whole extracted teeth with different excavation methods, was compared. Drilling with a high-speed bur and chemo-mechanical excavation (Carisolv, RLS Global AB, Gothenburg) after stepwise staining and excavation were examined with a Leica M80 Stereo Microscope (Leica M80 with 8:1 zoom, x0.75, Leica Mikrosysteme Vertrieb GmbH) and photographed by a Leica digital camera (Leica DFC420 C, Leica Mikrosysteme Vertrieb GmbH, equipped with Leica Application Suite LAS V3.7.0 Leica Microsystems AG),.

### **3.3.6 A systematic review of deciduous dentition using Carisolv or burs (Paper IV)**

#### **The focused PICO questions**

The systematic review followed the guidelines of the Transparent Reporting of Systematic Reviews and Meta-Analyses.<sup>147</sup> The following focused PICO questions were set; what is the effect of using Carisolv on primary teeth for caries excavation compared with the traditional drilling technique regarding a) caries removal rate (clinically appreciated), b) clinical efficiency (treatment time) and c) patient comfort (need for anaesthesia).

#### **Eligibility criteria**

The study inclusion criteria for this review were clinical trials; randomised clinical trials and controlled trials aiming to evaluate the efficacy on the primary dentition using Carisolv or a traditional drilling instrument (control). The eligibility criterion was total caries removal without any time limit in each group. Furthermore, studies assessing complete caries removal outside common practice such as using a sharp probe were excluded. However, studies with the additional experimental groups to Carisolv or burs were included.

#### **Search strategy**

For the identification of studies to evaluate for this review, a unique search strategy to be applied to each database research was developed using the following key words: Carisolv and Chemo mechanical Caries Removal. No Mesh term matching Carisolv was found.

Database research was conducted using MEDLINE via PUBMED (from 1948 to December 2014), Web of Science (from 1948 to December 2014), and COCHRANE database SCOPUS (from 1969 to December 2014).

Two separate authors were charged with evaluating the eligibility of the studies and independently examined all the abstracts in the selected papers. If an abstract did not supply enough information to determine whether the paper met the inclusion criteria, a full report was obtained. The two authors assessed the papers independently in order to establish whether or not the studies met the inclusion criteria. All the studies which appeared to meet the inclusion criteria were obtained in full-text format.

### **Data analysis**

The resulting data obtained from the studies answered the PICO questions on complete caries removal (binary yes/no), time taken (continuous) and pain threshold during the procedure, i.e. the need for anaesthesia by patients (binary yes/no). When raw data were not available in the text, tables or graphs, the author was contacted to obtain this information. A meta-analysis was conducted for all studies, interventions and outcome measurements. To compare dichotomous data, a calculation of the odds ratio (OR), along with 95% confidence intervals (CIs), was used, whereas, for continuous data, the mean difference (MD) with 99% confidence intervals (CIs) was calculated. The Z-test was also used for each comparison. A random-effects model was applied to reassess all the data extracted from the included studies. Analysis was performed using Review Manager 5.3 software provided by the Cochrane Collaboration [Review Manager (RevMan)-Version 5.3.2012].

## 4 RESULTS

### 4.1 Chemical alterations in carious tissue

Fourier Transform Infrared Spectrum (FTIR) enables analyses of chemical alterations in powdered form, without further purification. This was considered in Paper I.

From the FTIR-KBr analysis in Paper I (*Part I*) none of the samples, sound dentine *S01-SD*, *S02-SD*, carious inner dentine *S03-ICL*, *S04-ICL* and carious outer dentine *S05-OCL*, *S06-OCL* exhibited a distinct ester carbonyl {C=O stretch} absorption peak around  $1740\text{ cm}^{-1}$  in the deconvoluted spectra. (FIGURE 11).

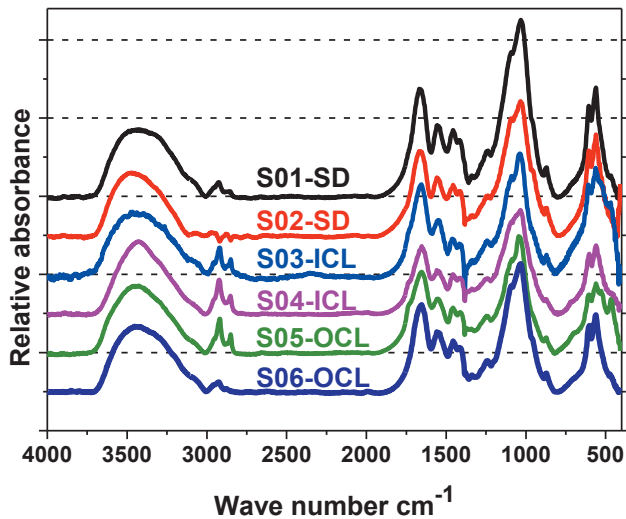


Figure 11. Deconvoluted FTIR spectra from  $4000\text{-}500\text{ cm}^{-1}$  of sound dentine *S01-SD* and *S02-SD* (*Part I*) carious dentine from the inner layer *S03-ICL* and *S04-ICL* in *Paper I*

However, shoulders were observed around  $1740\text{ cm}^{-1}$  in the characteristic peak position of the ester carbonyl group for the inner layer **S03-ICL**, **S04-ICL** and in one of the outer layers **S05-OCL** (FIGURE 11).

After spectral subtraction with sound dentine **S02-SD**, peaks were seen in all the carious samples, **S03-S06**, with largest amount in the carious inner dentine, **S03-ICL**, at  $1739\text{ cm}^{-1}$  and  $1736\text{ cm}^{-1}$ , respectively (FIGURE 12). Similar results were also found in *Part II S10* and *Part III S13*, respectively (FIGURE 13). Carious dentine exhibits absorbance in the region of carbonyl esters at  $1740\text{ cm}^{-1}$  using FTIR-ATR, whereas no shoulder was detected for the sound dentine sample **S01-D**.

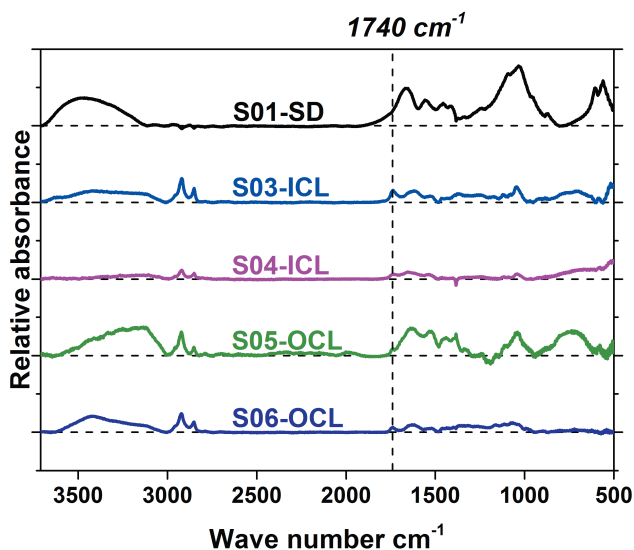


Figure 12. FTIR spectra of the amide I band (Part I), representing carious tissue from the inner layer **S03-ICL** & **S04-ICL** and outer layer **S05-OCL** & **S06-OCL** after the subtraction of sound dentine in Paper I. The shoulders at  $1740\text{ cm}^{-1}$  representing ester functions are marked with a dotted vertical line.

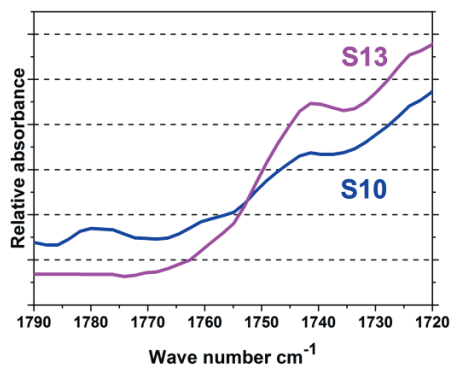


Figure 13. Enlargement of the region of  $1790\text{-}1720\text{ cm}^{-1}$  from the FTIR-ATR spectra of the untreated inner layer of carious dentine from Part II **S10** and Part III **S13** showing the ester function of carious dentine.

In the spectral region  $1800\text{-}400\text{ cm}^{-1}$  (Paper I, *Part III*), as illustrated in FIGURES 13b and d, four unique absorbencies for carious dentine **S10-S12** were found at  $1740\text{ cm}^{-1}$  {carbonyl esters C=O},  $1340\text{ cm}^{-1}$  {C-H deformation; C-N stretch of primary, secondary and tertiary aromatic amines},  $1286\text{ cm}^{-1}$  {C-H deformation} and  $1210\text{ cm}^{-1}$  {C-C(=O)-O stretch} compared with sound dentine **S07-S09**. FIGURE 14A. In addition the bands at  $1286$  and  $1210\text{ cm}^{-1}$  appeared enlarged after reaction with the hydrazine derivative (=Lucifer yellow) **S11**, **S12** in comparison with the caries reference sample **S10**. (FIGURE 14 B). Moreover samples **S11**, **S12** show that the spectral features associated with the carbonyl esters {C=O} at  $1740\text{ cm}^{-1}$  were changed, i.e. reduced or lost in contrast to sound dentine **S10** (FIGURE 14B).

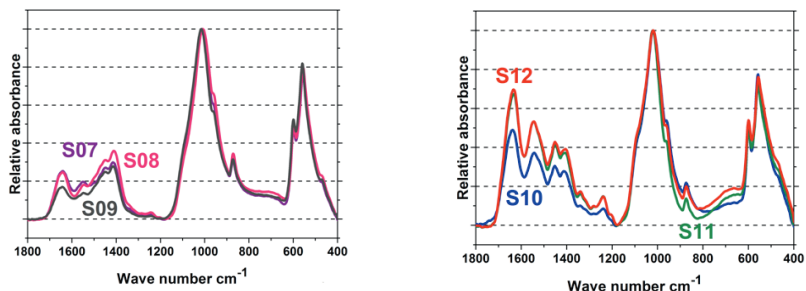


Figure 14. *a-b*: FTIR-ATR spectra (Part III), of sound dentine (*a*) and of carious dentine (*b*) in Paper I. Unique absorbances for carious dentine **S10-S12** compared with sound dentine **S07-S09** were found at  $1740\text{ cm}^{-1}$ ,  $1340\text{ cm}^{-1}$ ,  $1286\text{ cm}^{-1}$  and  $1210\text{ cm}^{-1}$ .

When comparing the amide I band at  $1650\text{ cm}^{-1}$  with the phosphate band at  $1100\text{ cm}^{-1}$  of sound dentine (FIGURE 13A) and of carious dentine, an interesting difference in the mineral/protein ratio was observed, with lower values for the carious dentine (FIGURE 14A). The lower region of the spectra, the amide I band, was shifted from  $1660\text{ cm}^{-1}$  for sound dentine to  $1650\text{ cm}^{-1}$  for carious dentine (FIGURE 14B). A shift in the intensity from the sound dentine **S07-S09** and the carious dentine **S10-S12** at  $1450\text{ cm}^{-1}$  and  $1417\text{ cm}^{-1}$  was also found (FIGURE 14B).

## 4.2 Binding properties with Lucifer yellow

A carious sample treated with Lucifer yellow (hydrazine derivative) was analysed with ToF-SIMS in Paper I (Part III) viewed in (FIGURE 15). The spectra showed that the reference spectra of carious dentine had the largest mass fragment at  $652.56\text{ mass/charge (}m/z\text{)}$ , whereas after the staining with Lucifer yellow it contained masses up to  $1505.56\text{ }m/z$ . Greater masses were thus detected after the reaction between Lucifer yellow and carious dentine **S15** than before **S13** (FIGURE 15). Moreover, fragmentation was observed

after the reaction between Lucifer yellow and carious dentine **S15**, where 106 mass units were repeatedly lost. This was not found for sound dentine after the Lucifer yellow treatment. No differences before or after the treatment of sound dentine with Lucifer yellow were observed Paper I. ToF SIMS analysis of Lucifer yellow revealed no masses greater than 600  $m/z$ .

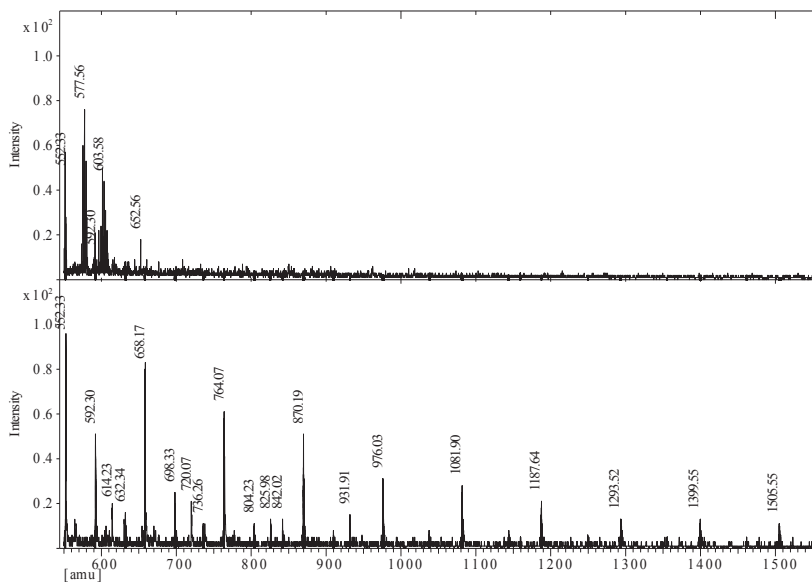


Figure 15. The positive TOF-SIMS spectra ( $m/z$ ) Part III, in Paper I of the inner layer of carious dentine before **S13** and after **S15** treatment with NaOH/ Lucifer yellow.

To verify the binding properties of Lucifer yellow to carious dentine a  $^{15}\text{N}_2$ -hydrazine was used as a simple molecular model of Lucifer yellow in Paper III. From the positive TOF-SIMS spectra the main contribution at the  $m/z$  34.03 derives from  $\text{H}_2^{15}\text{N}-^{15}\text{NH}_2$  and is therefore the most important peak for measuring hydrazine in the stained dentine (TABLE 4). In the negative ToF-SIMS spectra on the other hand the peak at  $m/z$  27.00 mainly contained a contribution from  $\text{C}^{15}\text{N}$  fragments (in addition to  $^{13}\text{CN}$ , HCN).

Table 4. Occurrence of the main contributed mass fragments in normal {ND} and carious dentine {CD} after staining with hydrazine {HY}, Lucifer yellow {LY} and with  $^{15}\text{N}_2$ -hydrazine-labelled Lucifer yellow {HY•LY}. Normal dentine stained with hydrazine after one washing procedure (ND-HY-1); and after a second washing procedure (ND-HY-2); carious dentine stained with hydrazine after one washing procedure CD-HY-1); and after a second washing procedure (CD-HY 2); carious dentine stained with partly  $^{15}\text{N}_2$ -labelled Lucifer yellow (CD-LY•HY).

## ToF-SIMS

## 34.03 m/z (H215N-15NH2): positive mode

ND	ND-HY-1	ND-HY-2	HY•LY
0±0	1.30±0.45	0.34±0.13	360.00±166.00
CD	CD-HY-1	CDHY-2	CD-HY-LY
0.31±0.03	34.00±5.90	15.00±2.80	0.79±0.03

## 27.00 m/z 27.00 (C15N): negative mode:

ND	ND-HY-1	ND-HY-2	HY•LY
0.19±0.03	0.52±0.03	0.21±0.04	2.80±0.32
CD	CD-HY-1	CDHY-2	CD-HY-LY
0.32±0.30	1.40±0.19	0.67±0.09	0.36±0.10

The intensity (counts) at the  $m/z$  34.03 of carious dentine stained with hydrazine decreased with the number of washes from the first wash **CD-HY-1** to the second washing procedure **CD-HY-2**, shown in (FIGURE 16). The highest intensity ( $\approx 31$ ) was found for **CD-HY-1**, which was three times higher compared with **CD-HY-2** ( $\approx 11$ ). Unstained carious dentine **CD** and normal dentine stained with hydrazine after a second washing procedure **ND-HY-2** only reached an intensity value of 2. The relative intensity of hydrazine-stained carious dentine **CD-HY-2** was considerably higher compared with stained normal dentine **ND-HY-2** (TABLE 4 and FIGURE 16). Moreover, the relative intensities for carious dentine **CD** at the peaks of 34.03 and 27.00 were all higher compared with normal dentine **ND**, indicating changes in the dentine caused by the caries process (TABLE 4 and FIGURE 16).

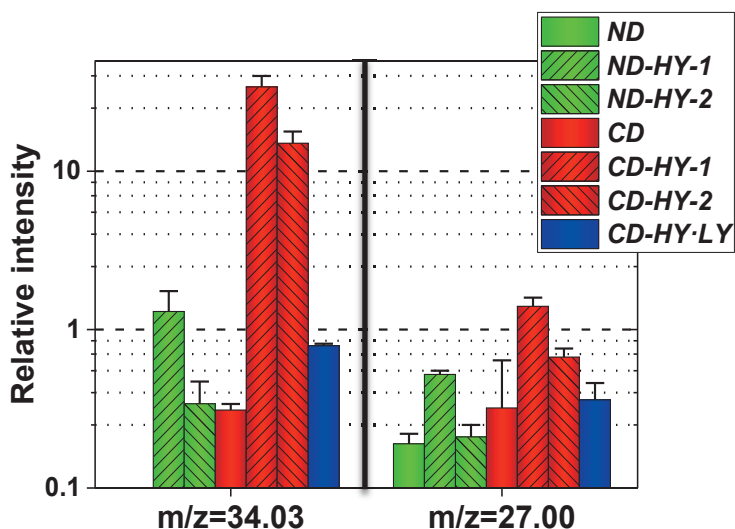


Figure 16. The relative intensities ( $\text{Log}_{10}$ ) of the mass-to-charge ratio ( $m/z$ ) from the ToF-SIMS analyses for the peaks of 34.03 (Pos mode) and 27.00 (Neg mode) respectively. Normal and carious dentine (ND=normal dentine; CD=carious dentine). Hydrazine-stained normal and carious dentine after one washing procedure and carious dentine stained with  $^{15}\text{N}_2$ -hydrazine-labelled Lucifer Yellow (ND-HY-1=normal dentine; CD-HY-1=carious dentine; CD-HY-LY=carious dentine). Hydrazine-stained normal and carious dentine after two washing procedures and carious dentine stained with  $^{15}\text{N}_2$ -hydrazine-labelled Lucifer Yellow (ND-HY-2=normal dentine; CD-HY-2=carious dentine; CD-HY-LY=carious dentine).

### 4.3 Binding properties with hydrazine

$^{15}\text{N}$  NMR spectra were obtained for carious dentine treated with hydrazine,  $\text{H}_2^{15}\text{N}-^{15}\text{NH}_2$ , **CD-HY-2** and **CD-HY-1** to confirm presumed covalent bonding to the carbonyl groups of carious dentine. The  $^{15}\text{N}$  CP spectrum revealed four resonances at around 50, 105 and 125 ppm and at 173 ppm. The resonances were assigned to  $^{15}\text{N}$  bound to carbonyl groups and the corresponding molecular structures are depicted in FIGURE 17.

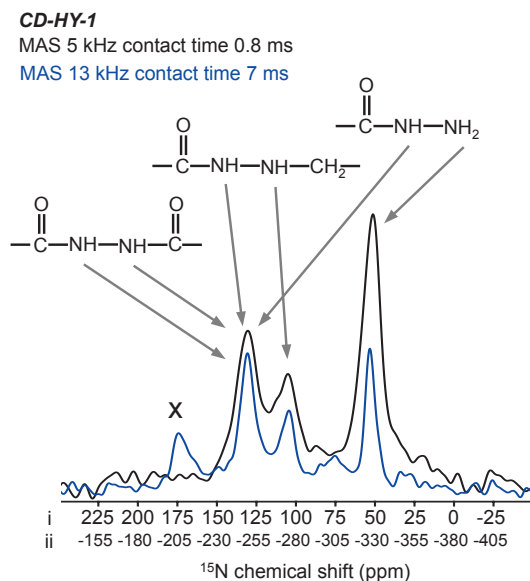


Figure 17.  $^{15}\text{N}$  CP MAS spectra of carious dentine stained with hydrazine after one washing {CD-HY-1} at a 5 kHz MAS rate, a contact time of 0.8 ms (black), a 13 kHz MAS rate and a contact time of 7 ms (blue) respectively. Two  $^{15}\text{N}$  chemical shift scales are shown referenced to liquid  $\text{NH}_3$  (i) and to  $\text{CH}_3\text{NO}_2$  (ii).

To ensure that the observed  $^{15}\text{N}$  resonances arise from covalently bound nitrogen atoms, the CD-HY-1 sample was washed extensively for a second time and dried CD-HY-2. The  $^{15}\text{N}$  CP spectra of both CD-HY-1 and CD-HY-2 are shown in FIGURE 18 (bottom) and all  $^{15}\text{N}$  signals were still observed after the second washing step. Furthermore no detectable  $^{15}\text{N}$  signal was observed for the additional  $^{15}\text{N}$  CP spectrum of normal dentine ND and carious dentine CD as shown in FIGURE 18 (top).

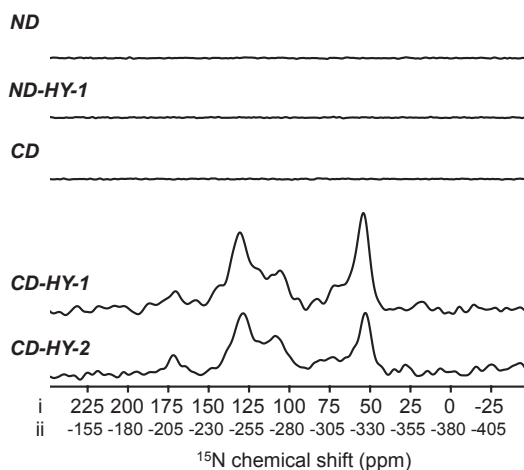


Figure 18.  $^{15}\text{N}$  CP MAS spectra of normal dentine **ND**, normal dentine stained with hydrazine and after the first washing procedure **ND-HY-1**, carious dentine **CD**, carious dentine stained with hydrazine and after the first washing procedure **CD-HY-1** and after the second washing procedure **CD-HY-2** at a 5 kHz MAS rate and contact time of 1 ms. Two  $^{15}\text{N}$  chemical shift scales are shown referenced to liquid  $\text{NH}_3$  (i) and to  $\text{CH}_3\text{NO}_2$  (ii).

## 4.4 Visualisation of the covalent binding with hydrazine

Stereomicroscopic observations of sagittal uncalcified sectioned teeth exposed to dyes with different binding properties, such as Food blue (FB) and Acid red 1 (AR), for electrostatic binding properties, and amino fluorescein (AFS), Lucifer yellow potassium salt (LYCH) and Alexa fluor 594 (AF594), for both covalent and electrostatic binding properties, showed that the covalent dye binds to carious dentine in (Paper II). The covalent properties originate from the hydrazine part of the dyes that, after binding to carbonyl ester, form a covalent bond to the carious tissue in (Papers I-III).

Stereomicroscopic observations of sagittal un-calcified sectioned teeth exposed to dyes with different binding properties such as Food Blue (FB) and Acid Red 1 (AR) of electrostatic binding properties and Amino Fluorescein (AFS), Lucifer Yellow potassium salt (LYCH), Alexa Fluor 594 (AF594), of both covalent and electrostatic binding properties showed the covalent dye to bind to carious dentine. In Paper II .The covalent properties originate from hydrazine part of the dyes that after binding to carbonyl ester form a covalent bond to the carious tissue in Papers I-III.

To be able to exclude the effect of different concentrations all dye solutions were performed within the same concentration (15 mM). The long exposure time of 24 hrs enabled the reactions to reach chemical equilibriums for the different treatments. (Flow chart in FIGURE 9). From the following microscopic analysis, it was deduced that dyes still remaining after the competitive reaction of the high ionic strength i.e. after the competitive reaction of the high ionic strength (NaCl, 1 M) and from the additional strong basic solution (NaOH, 0.5 M) must be covalently attached to the tooth cavity. Dyes not attached to the cavity after the basic solution treatment was deduced to be of electrostatic character (FIGURE 19). Furthermore, it was found that healthy tissue was not stained by the hydrazine dye (FIGURE 20-21 d).

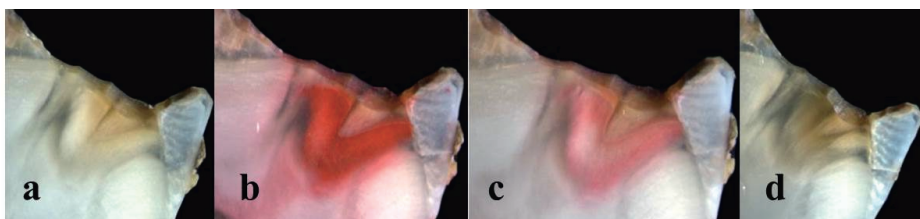


Figure 19. Staining with Acid red (210633, Aldrich, USA) at initial (a), dye treatment 24h (b), NaCl (1 M) treatment (c), and NaOH (0.5 M) treatment (d) during 24h.

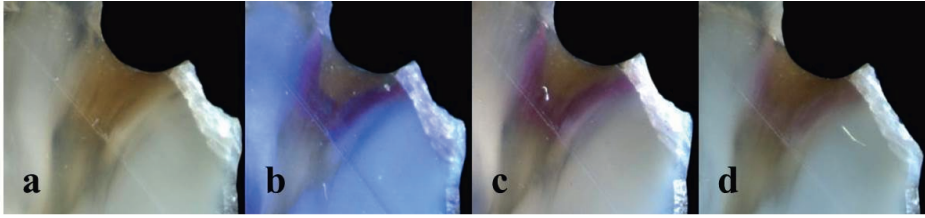


Figure 20. *Figure a-d: Staining with Alexa fluor 594 (A10438, Life technologies, USA) at initial (a), dye treatment 24h (b), NaCl (1M) treatment (c) and NaOH (0.5M) treatment (d) during 24h.*

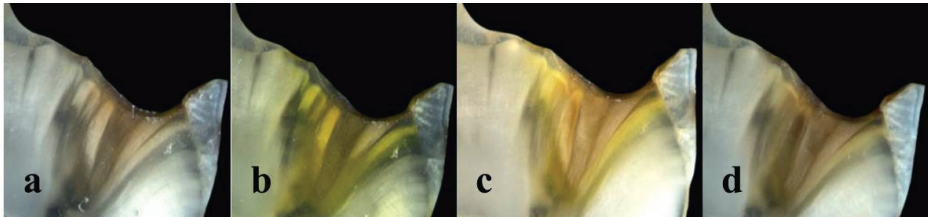


Figure 21. *a-d Staining with Lucifer yellow (L0144, Sigma, USA) at initial (a), dye treatment 24h (b), NaCl (1M) treatment (c) and NaOH (0.5M) treatment (d) during 24h.*

## 4.5 Visualisation of the covalent binding after chemo-mechanical excavation

The application of a mixed solution with hydrazine, food blue and lucifer yellow CH, on whole caries-affected teeth showed that hydrazine stains carious dentine in a specific manner. After the cavity floor was prepared either using the chemo-mechanical technique or with burs until a caries-free surface was obtained, a second staining showed that the dentine was not completely caries free after chemo-mechanical excavation (FIGURE 22), whereas the hydrazine based dye appeared to have stained the smear layer

from the drill excavation (FIGURE 23). The excavation technique therefore appeared to affect the staining properties by mechanical means.

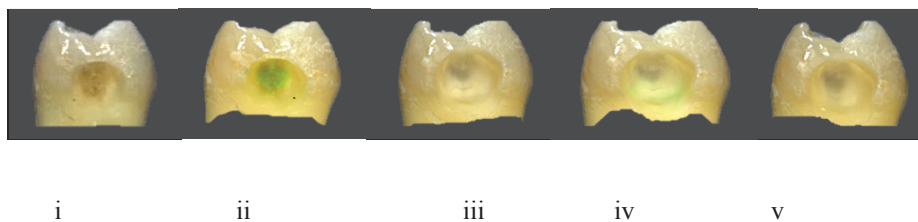


Figure 22. Digital images of whole teeth with open carious dentine cavities at the start (i), after staining with FB+LYCH for 30 s (ii), after rinsing and excavation with a high-speed bur (iii), after a second staining for 30 s and rinsing (iv) and after final excavation with a high-speed bur and a third staining for 30 s and rinsing (v)



Figure 23. Digital images of whole teeth with open carious dentine cavities at start (i), after staining with FB+LYCH after staining for 30 s (ii), after rinsing and excavation with a high speed bur (iii), after second staining for 30 s and rinsing (iv), and after final excavation with a high speed bur and a third staining for 30 s and rinsing (v).

Digital images of whole teeth with open carious dentine cavities at start (i), after staining with FB and LYCH after staining for 30 s (ii), after rinsing and excavation with a high speed bur (iii), after second staining for 30 s and rinsing (iv), and after final excavation with a high speed bur and a third staining for 30 s and rinsing (v).

## 4.6 Systematic review of traditional burs vs. chemo-mechanical caries removal

The purpose of the systematic review and meta-analysis was to evaluate the reliability of the Carisolv system with respect to drilling regarding the full removal of decayed hard tissues in primary dentition. In addition, the maximum time for caries removal and finally the overall effect were compared.

The search strategy from PubMed, Scopus and ISI-web Knowledge databases resulted in a total of 195 unique articles published from 1999–2014 being identified and assessed. Twenty-eight papers were analysed and 10 studies finally met the eligibility criteria. Furthermore, the trials included a total of 348 patients and 532 treated teeth. Six of the trials included only primary teeth, with the age of the participants ranging from 28 months to 11 years.

Complete caries removal was obtained in 100% (151 of 151) of decayed teeth using Carisolv and 99.2% (112 of 113) using the drill. When combining the data in the meta-analysis, the summary OR was 0.33 (99% CI = 0.00–22.65). Data were obtained from three papers with a total of 264 analysed teeth. However, there was no statistical difference in caries removal between the chemo-mechanical system (Carisolv) and the rotary instrument ( $z=0.68$   $p=0.50$ ) based on the evidence.

The calculation of the time required (in seconds, s) to complete the procedure was based on seven studies involving a total of 480 teeth. The maximum time required for caries removal was 648.0 s for Carisolv and 206.7 s for the rotary instrument, whereas the minimum time of treatment was 402.0 s and 80.7 s respectively.

The z-test for overall effect for the Carisolv group vs. rotary instruments was  $z = 10.49$ ,  $p < 0.01$ . The z-test for overall effect for the Carisolv group vs. rotary instruments was  $z = 10.49$ ,  $p < 0.01$ .



## 5 DISCUSSION

The chemical alterations (esters) found in this thesis solely belong to the carious tissue, not seen in sound dentine. In addition these are possible to “mark” after reaction with specific dye. From a clinical perspective, this might be useful, as it would distinguish affected tissue from healthy tissue during restorative work.

The work resulted in three papers. Paper I revealed a unique functional group in carious tissue that was subsequently able to react with a specific dye used in further studies in Paper II. The reactive part of the dye was proven to bond covalently (strongly) to the unique groups of carious dentine revealed in further studies Paper III. Paper IV summarised clinical studies of the chemical and mechanical removal of carious tissue on primary teeth, where the chemically based product, Carisolv, appeared to enable effective excavation within the paediatric working field. The product is a good alternative to mechanical excavation, as it works by de-attaching the necrotic tissue that contains the unique groups of carious dentine.

### Identifying the chemical alterations in carious tissue

Esters are normally formed in nature from reactions between structures holding alcohol functions and carboxylic acids, most often acid catalysed.<sup>80, 102</sup> The formation of esters is influenced by water and changes in acidity.<sup>80, 102</sup> The reduction in the water content in parallel with pH changes going from the outer to the inner part of a lesion.<sup>35, 148</sup> would favour ester formation in a cavity. Moreover, the presumed presence of ester functional groups in carious dentine has previously been suggested to arise from acylated hydroxyl groups in carious dentine, which modify the tissue to a collagenase-resistant form.<sup>68</sup> It is also suggested that ester groups derive from bacterial lipid components in both sound and carious dentine.<sup>79</sup> and larger amounts of esterases have been found in carious tissue compared with sound tissue, respectively.<sup>78</sup> Although ester functions are extremely common in biological soft tissues, especially in altered tissues such as synovial fluids or in carcinogenic active tissue,<sup>149, 150</sup> they have not as yet been reported in mineralised tissue.

The vast majority of techniques used for tissue analysis require protein extraction from the calcified tissue. It is a challenge to find a suitable

analytical analysis method for the determination of chemical alterations in carious tissue, as, to date, the tissue has had to be excavated with different techniques, followed by yet other techniques for the isolation of the alterations.<sup>45</sup> However, both FTIR and ToF-SIMS have previously been proven to be useful for the determination of chemical alterations in hard tissue, without extensive sample preparation and protein purification.<sup>26, 33, 72, 132</sup> Studies of powdered teeth are less frequent, but they have been shown to be useful in analysing the phospholipid content of peritubular dentine.<sup>75</sup> Nevertheless, limited research has been performed on powdered dentine and carious dentine for the determination of the chemical composition.

Because of the minimum of tissue preparation required, thereby minimising the risk of hydrolysis, both FTIR and ToF- SIMS were therefore chosen as the primarily analytical tool in Paper I and Paper III. The excavation technique used for the different samples can be questioned, as it must be regarded as fairly crude, based on visual and tactile judgement. However, all the samples were collected by one of the authors, also an experienced dentist, under standardised conditions similar to normal excavation techniques at the clinic.

From both the deconvoluted IR spectra and the subtraction IR spectra in Paper I, it was concluded that ester groups, at  $1740\text{ cm}^{-1}$  at the amide I band, displayed a greater presence in the inner layer of carious dentine compared with the outer layer of carious dentine. No esters were seen in the sound tissue. The resulting peak found at  $1739\text{-}1736\text{ cm}^{-1}$  of the inner and outer layer of carious dentine corresponds to the known characteristic peak position of the ester carbonyl group.<sup>137</sup> The second characteristic absorption region of esters at  $1300\text{-}1050\text{ cm}^{-1}$  was more difficult to interpret, as other functional groups also absorb in that region. Furthermore, to avoid the appearance of false peaks in the deconvoluted spectra, a subtraction technique was used on each FTIR spectrum with the result of true peaks. This means that, when subtracting healthy dentine from carious dentine, unique peaks of the carious dentine appear and, as a result, the presence of carbonyl groups (C=O) could be observed. Normally, saturated esters absorb between  $1750\text{ and }1735\text{ cm}^{-1}$ , suggesting that the signals viewed in the subtraction spectra at  $1739\text{-}1736\text{ cm}^{-1}$  correspond to absorptions from normal saturated esters.<sup>137</sup> In addition, amino acid esters arising from lactones are prescribed to absorb at  $1735\text{-}1720\text{ cm}^{-1}$  by IR (KBr) and could therefore also be part of the signals observed at  $\sim 1740\text{ cm}^{-1}$ .<sup>137</sup>

The following FTIR-ATR analysis revealed unique peaks for carious dentine at 1740, 1340, 1286 and 1210  $\text{cm}^{-1}$ , not observed in sound dentine, although some absorbances, such as those at 1450  $\text{cm}^{-1}$  and 1417  $\text{cm}^{-1}$ , were the same, but with different intensities, indicating differences between these two tissues.

Moreover, collagen (the major protein in dentine) is reported to exhibit a series of unique IR absorptions between 1300 and 1000  $\text{cm}^{-1}$ .<sup>130</sup> This could possibly explain the absorbances of C-C(=O)-O stretch at 1210-1190  $\text{cm}^{-1}$  and/or 1299-1250  $\text{cm}^{-1}$ , unique to carious dentine found in Paper I. The peak at 1338  $\text{cm}^{-1}$  has been reported to be linked to the degradation of collagen<sup>47</sup> or to represent peaks of free amino acids at 1417, 1286 and 1210  $\text{cm}^{-1}$ .<sup>137</sup> The 1340  $\text{cm}^{-1}$  absorbance could be related to {C-O}-stretches of COOH (free amino acid) or of an ester.<sup>137</sup> It is also suggested that the higher absorbance at 1450  $\text{cm}^{-1}$  for the carious dentine is a consequence of an increase in the number of aliphatic side-groups of various amino acid residues.<sup>151</sup> These bands have been reported to belong to a  $\text{CH}_2$ -bending vibration at 1450  $\text{cm}^{-1}$  and 1406  $\text{cm}^{-1}$ .<sup>72</sup> Furthermore, the peaks at 1740, 1286 and 1210  $\text{cm}^{-1}$  also appeared to be affected by the reaction. The observed decrease in the absorbance of the carbonyl ester at 1740  $\text{cm}^{-1}$  after the treatment of the carious dentine with the hydrazine derivative suggests that a reaction has taken place in the ester group. The enhancement of the spectrum in the region about 1800-1700  $\text{cm}^{-1}$  implies that an amide-forming reaction has taken place between carious dentine and the hydrazine derivative, as the spectral features associated with the carbonyl esters {C=O} at 1740  $\text{cm}^{-1}$  were changed, i.e. reduced or lost. In addition, the absorbances of the new amides formed in the reaction between the esters and the hydrazine derivative would be hidden under the amide bands at 1650, 1550 and 1250  $\text{cm}^{-1}$ . The 286 and 210  $\text{cm}^{-1}$  bands are more difficult to predict. Moreover, the FTIR spectrum of Lucifer yellow shows strong absorbances at 230-120  $\text{cm}^{-1}$  and at 600-500  $\text{cm}^{-1}$  (not shown) and they are in the region of both the amide I band and at the strong absorbance of the mineral peaks.

Lucifer yellow (a fluorescent hydrazine derivative) was used in Papers I, II and III for its capacity both to form a new peptide and to visualise the reaction with the ester group in carious dentine.

### **Binding properties of Lucifer yellow to carious tissue**

ToF SIMS analysis of the powdered carious dentine treated with Lucifer yellow revealed larger masses after the treatment than before compared with the non-treated carious tissue in Paper I. The largest mass fragments of tested moieties were found in the positive spectra of the inner layer of carious dentine after reaction with hydrazine derivative at 975, 1081, 1187, 1293, 1399 and 1,505  $m/z$ . By rinsing with sodium hydroxide prior to analysis, unwanted hydrogen bonding between the tissue and the hydrazine derivative was avoided. Any possible bonding with the tissue must therefore be of a stronger character. The ToF-SIMS data also indicated that the untreated inner layer of carious dentine contains masses at 652.56  $m/z$ , whereas treated carious dentine contains masses over 1500  $m/z$  that strongly indicated that the hydrazine derivative is covalently bound to the tissue. In addition, the repeated loss of mass fragments at 106  $m/z$  was deduced to  $C_5NO_2$ , from the covalent binding of the hydrazine derivative to the carious tissue. This pattern was not detected for the sound dentine or the untreated carious samples respectively Paper I (FIGURE 6B).

Powdered samples of sound and carious dentine contain both mineral and proteins and treatments with an alkaline solution would therefore have the same effect on both these tissues. There is, however, a difference in fragmentation and mass content after treatment with Lucifer yellow, suggesting that a reaction has occurred in carious dentine and that the observed mass difference for the carious dentine treated with hydrazine derivative could not be due to the alkaline treatment. In the case of sound dentine, the positive mass spectra were similar for both the treated and untreated sound dentine samples respectively (In Paper I FIGURE 6B). Furthermore, both samples contained repeated mass differences between the mass peaks of 56  $m/z$  that were correlated to CaO. However, all the resulting mass fragments of healthy dentine were much larger (596 to 1300  $m/z$ ) than the mass of intact Lucifer yellow (521 g/mol), which suggests that Lucifer yellow did not react with the healthy dentine in (Paper I, FIGURE 6B) Accordingly, the Lucifer yellow selectively reacts with carious dentine tissue.

## Binding properties of hydrazine ( $^{15}\text{N}_2$ ) to carious tissue (CO and CN)

Isotopes such as  $^{15}\text{N}$  are easily identified by ToF-SIMS, which is thereby a useful analytical technique for studying the incorporation of  $^{15}\text{N}$ -labelled hydrazine derivate into carious dentine.

The ToF-SIMS data in Paper III for carious dentine stained with  $^{15}\text{N}_2$ -hydrazine and  $^{15}\text{N}_2$ -hydrazine labelled Lucifer yellow revealed a higher occurrence of  $^{15}\text{N}$  containing fragments compared with sound dentine *ND* or untreated carious dentine *CD*, showing a difference in staining reaction. One likely explanation could be that reactive functionalities of carbonyl types in carious dentine have reacted with  $^{15}\text{N}_2$ -hydrazine or the  $^{15}\text{N}_2$ -hydrazine chain in Lucifer yellow, as both stains have similar reactivity. The results support the findings in Papers I and II.

From the calculation of the intensities (counts) of the mass at 34.03 *m/z* (in Pos. mode), representing hydrazine, and 27.00 *m/z* (in Neg. mode), representing CN (amine), it is concluded that *CD-HY-1*, *CD-HY-2* and *CD-HY-LY* all had numerous intensities compared with untreated carious dentine. In addition, the washing procedure reduces the binding to carious tissue, which could be due to unspecific hydrogen bonding or an excess of hydrazine prior to washing. The abundance of *m/z* corresponding to hydrazine in untreated carious tissue is more difficult to explain, especially as sound dentine did not indicate any mass at 34.03 *m/z*. It is plausible that the carious process affects the tissue and the reported  $^{15}\text{N}_2$  masses originate from other aggregates formed under the ionisation event of ToF-SIMS. Moreover, hydrazine seemingly binds to sound dentine *ND-HY-1*, albeit weakly, as it could be washed away *ND-HY-2*.

NMR spectroscopy has become a standard analytical technique for studying biomaterials.<sup>40, 152-154</sup> More recently  $^{13}\text{C}$  NMR and  $^{15}\text{N}$  NMR in the solid state for observing structural changes in teeth tissues.<sup>133-134</sup> The NMR analysis in Paper III aimed to find the binding between the ester carbonyl groups of carious dentine and the  $^{15}\text{N}$ -hydrazine molecule *HY* in forming the reactions product an enriched  $^{15}\text{N}$ -amide. The  $^{15}\text{N}$  NMR analyses of hydrazine-stained carious dentine, after the second washing procedure *CD-HY-2*, revealed four resonance areas of interest at 50, 105, 125 and 173 ppm. The resonance signal at 50 ppm most probably arises from one  $^{15}\text{NH}_2$  end-group of the hydrazine molecule.<sup>155</sup> In the reaction between hydrazine and carious dentine. A hydrazine molecule has two reactive  $^{15}\text{NH}_2$  groups that could both react with acyl derivatives (esters) in the carious dentine, resulting in a

monoacylated and a diacylated hydrazine derivative, which both exhibit resonances at about 125 ppm.<sup>155, 156</sup> The <sup>15</sup>N-resonance signal from an amide function like this should appear at about 125 ppm. The signal at 104 ppm has the position of nitrogen connected to an alkyl group that has most probably been formed in a nucleophilic reaction on a carbon of an aliphatic phosphoric<sup>48</sup> or carbonic ester in the carious dentine. It is suggested that the resonance at 173 ppm is suggested to corresponds to the functional imine group like a Schiff base function, N=C, as in a structure H<sub>2</sub>N-N=CR(H)-,<sup>156</sup> which can be formed from hydrazine and aldehydes or ketones, present in the carious dentine in a similar reaction that initiates the formation of the Maillard product found in carious dentine.<sup>69-70</sup> The sugar acetals in the dentine are masked aldehyde functions. None of these four observed resonance signals was detected in the normal dentine after treatment with <sup>15</sup>N<sub>2</sub>-hydrazine.

The <sup>13</sup>C NMR analyses carried out after the staining of carious dentine with <sup>15</sup>N<sub>2</sub>-hydrazine labelled Lucifer yellow revealed resonances at 100-160 ppm for <sup>13</sup>C aromatic carbons in stained carious dentine, proving that the <sup>15</sup>N<sub>2</sub>-hydrazine labelled Lucifer yellow binds to carious dentine. No aromatic <sup>13</sup>C resonance could be detected in <sup>13</sup>C NMR after the treatment of sound dentine with Lucifer yellow, which is in agreement with the results in earlier observations in paper I. Furthermore, resonances from 20-80 ppm (solid state <sup>13</sup>CNMR, reference trimethyl silane) suggest that the peaks to originate from collagen molecule.<sup>40</sup>

When combining the results of the ToF-SIMS analysis with the NMR analysis, it seems very likely that the mass fragments observed from ToF-SIMS analysis can be traced in the <sup>15</sup>N NMR, like the N-acyl, N-diacyl or hydrazine chemical shifts detected by <sup>15</sup>N NMR. As a result, the <sup>15</sup>N NMR and the ToF-SIMS analyses support one another and it can be suggested that the covalent binding of the <sup>15</sup>N<sub>2</sub>-labelled hydrazine (<sup>15</sup>NH<sub>2</sub>-<sup>15</sup>NH<sub>2</sub>) has taken place in the carious dentine but not in the normal dentine. Only noise was found for the corresponding <sup>15</sup>N CP spectrum of hydrazine-stained sound dentine, proving that hydrazine does not bind to sound dentine.

### Visualisation of covalent binding with hydrazine

In order to be a helpful tool in the clinic, it is currently generally agreed that “The ideal caries-disclosing dye should solely stain the caries-infected but not the caries-affected dentine”<sup>90</sup> which explains why the selection of the

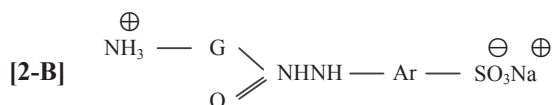
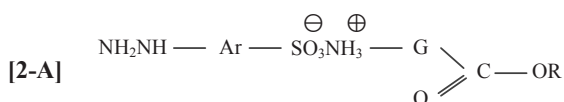
method used for this analysis is considered important. Since stereomicroscopy tends to over-score the lesion, the addition of dyes is claimed to be accurate and reliable in these analyses.<sup>86</sup> Consequently, stereomicroscopic analysis with digital photographs on sectioned lesions can be regarded as useful for the detection of dyes in dental hard tissues.<sup>61, 84</sup> In Paper I, it was found that a dye, such as Lucifer yellow, bound to carious dentine and subsequently more specifically with the hydrazine group of Lucifer yellow or with <sup>15</sup>N<sub>2</sub>-hydrazine. Hydrazine-based dyes can therefore be used as a stain to discriminate between normal and carious dentine. Based on the chemical and light-stereomicroscopic observations in Paper II stains with a covalent binding capacity were found to bind to carious dentine in contrast to dyes with only an electrostatic binding capacity, as they were proven to be still attached after the different treatments. To avoid the uncertainty associated with variations in biological tissues, the same tooth with manifest dentine caries was sectioned into five un-decalcified samples, during the staining procedure, thereby making it feasible to compare the staining capacity of different stains in basically the same tissue.

All the dyes used in Paper II have the potential to bind either to the acidic groups (NH<sub>3</sub><sup>+</sup>) or to the ester function groups (-COOR) of carious dentine. This results in the formation of a salt via an electrostatic bond [2-A] or an amide functional group [2-B]. The formation of an amide requires a longer reaction time than the formation of an electrostatic bond, which is immediate.

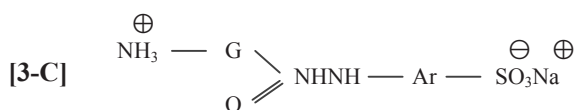
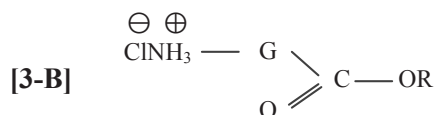
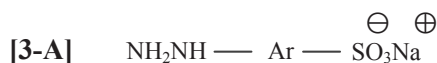
Acid red and food blue are only able to react in an electrostatic manner, as their binding groups are of an anionic character (SO<sub>3</sub><sup>-</sup>). They were therefore completely removed after the NaOH treatment. Alexa fluor 594 and Lucifer yellow both contain an electrostatic group (SO<sub>3</sub><sup>-</sup>) and a hydrazine derivate group (NH<sub>2</sub>NH-R) and, for this reason, they are able to react with both positive ions and the ester functions of the carious tissue. However, the hydrazine derivative, amino fluorescein, only contains hydrazine groups and may only react with the esters in a covalent manner, where the dyes resist all the different treatments. Mixtures of two stains, food blue (blue colour) with Lucifer Yellow CH (yellow colour) and Food Blue (blue colour) with Amino fluorescein (yellow colour), resulted in a green coloured solution. The green mixture became more bluish after the NaCl treatment. This indicates the yellow colour to be replaced by the (Cl<sup>-</sup>) ion in electrostatic part (SO<sub>3</sub><sup>-</sup>) and the blue colour to be stoichiomerically larger. After subsequent alkaline treatment the blue colour vanished and the yellow appeared. Thus, the small portion of the yellow colour seemed hidden under the blue colour that only have electrostatic binding properties. After the removal of all electrostatic bindings, only the yellow colour is left and must be covalently bonded. An in-house experiment (data not shown) showed that the yellow colour reacted



last reaction is thermodynamically favoured, as an amide is more stable than an ester.

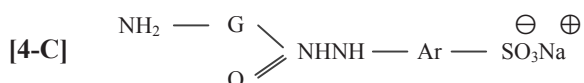
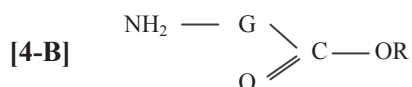
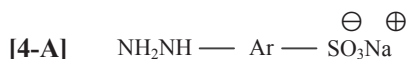


The addition of NaCl in a high concentration causes an ion exchange to occur in the electrostatic bond, thus exchanging  $\text{SO}_3^-$  for  $\text{Cl}^-$  in the stained carious dentine, structure [2-A], and consequently causing the removal of the stain from the carious tissue. The reaction products [3-A; 3-B; 3-C] are observed as a water-soluble un-attached stain in the supernatant [3-A], as de-stained hydrochloride salt of the carious dentine [3-B] and as stained carious dentine [3-C] respectively. As the ion exchange is an equilibrium reaction, all electrostatically bonded staining will not be removed in this way. The amide structure [2-B] will not be affected by the NaCl treatment.



In addition, as there is also an equilibrium relationship between structures [2-A] - [3-A] - [3-B] and the chloride ions ( $\text{Cl}^-$ ), some electrostatically bonded stain will still remain in the tissue. The final treatment with NaOH will deprotonate all the ammonium groups converting the stained carious dentine, represented as structures in [2-A], [2-B], [3-B] and [3-C] irreversibly to

structures seen in [4-A] (water soluble stain), [4-B] (unstained de-protonated carious dentine) and to stained carious dentine [4-C].



This indicates that the final removal of the electrostatically bonded dye will be carried out by the treatment with the NaOH solution, which will deprotonate the ammonium ion ( $-\text{NH}_3^+$ ). The positive charge for attracting the  $-\text{SO}_3^-$  group will therefore no longer be available. The electrostatically bonded dye will be fully released and transferred to the water solution as structure [1-B]. This was also observed from the high concentration of dye in the supernatants from the electrostatically stained tissue. The amide product as seen in [4-C] will not be affected by the sodium hydroxide treatment and the staining from the amide product will therefore remain in the tissue.

Furthermore, stains containing both electrostatically and covalently bonding groups will react with both an electrostatic structure [2-A] and a covalent bonding structure [2-B]. Treatment with NaCl and NaOH will therefore remove the electrostatically bonded part of the stain, while the amide-bonding part will be unaffected by both the NaCl treatment and the NaOH treatment.

### Visualisation of the covalent binding with hydrazine following chemo-mechanical excavation

After specific staining with the hydrazine derivative, excavation will take place. Consequently, the excavation technique may affect the specific

staining. Studies have found that chemo-mechanical excavation is more suitable for this staining procedure, as the prepared cavity floor could not be re-stained.<sup>157</sup> This is because there was no carious tissue left and a final endpoint was reached. For the treatment with the high-speed bur, a similar judgement of the prepared cavity floor was made; in spite of this, the prepared cavity surface became stained again. This is difficult to interpret because the cavities were judged to be completely caries free in both cases and the dyes are also specific to carbonyl modifications as esters. However, drilling forms a smear layer, which could presumably form ester functional groups, which explains why dyes are more suitable during chemo-mechanical excavation.

### **Chemo-mechanical excavation**

Carisolv was introduced in the dental market in Sweden in 1998 and has since been used for treatment in both the permanent and primary dentition. However, at present, most studies have been performed within paediatric dentistry. Paper IV, produced further insight into the reliability of the Carisolv system from a number of studies published between (1999-2014) with a total of 450 primary teeth involved.

The PICO questions addressed in the review comprise the efficacy of the chemo-mechanical treatment in terms of the complete caries removal rate compared with the traditional drilling technique, an evaluation of the treatment time and patient comfort defined as a need for anaesthesia. The removal rate was used as the efficacy parameter, even though it could be regarded as very subjective, as it is based on visual inspection and tactile control, but it is the most well known and used method.<sup>126, 136</sup> Caries detectors are an alternative, although there is scepticism about them in the literature.<sup>92, 95, 97, 98, 100</sup>

There was a significant difference regarding time required by the Carisolv procedure and the conventional drilling: treatment time was statistically significantly longer using Carisolv than drilling in 5 (7) clinical studies. The reason was the need of multiple applications of Carisolv gel, that seems to correlate with the cavity size (Chaussain-Miller).

Data on pain or need of local anaesthesia were reported in four papers. Carisolv reduced the use of local anaesthesia and the difference may be

related to the use of Carisolv gel, with the special designed hand instruments. However, it is necessary to consider that the four studies were heterogeneous in their design and the Carisolv group was more numerous than the control group. This corresponds well with previous studies<sup>104, 124, 125</sup> and is considered of particular interest during the treatment of children where extra care should be given in order to work as psychological as possible.

All Carisolv treatment takes longer time than the traditional method in removing carious dentine. The average difference in caries excavation time was in the present meta-analyses ( $z=10,49$ ,  $p < 0.01$ ) min. Depending on for example surface treated, lesion size and caries activity the treatment time may vary. A wide range in time difference between caries excavation using the chemo-mechanical technique and rotating burs have previously been shown. However, taking into consideration that anaesthesia often not may be needed the difference in time may not be so striking. The “total treatment time” may be a more accurate figure to be measured instead of only the time for caries excavation. Both the increased time and the less anaesthesia required by patients treated using the Carisolv were comparable.<sup>112</sup> In another review comparing the efficacy of caries removal, time and pain threshold, respectively, on primary teeth by using air-rotor, hand instruments, Carisolv and polymer burs. The Carisolv and polymer bur was found to be similar in caries removal effectiveness and could be considered as alternatives to painful procedures as air-rotor in management.<sup>111</sup>

Due to the heterogeneity among study designs and to the shortage of data the use of Carisolv limits to obtain an overall correlation among outcome variables, why there is the need of further large-scale, well-designed RCTs.

## CONCLUSION

The focus of the present thesis was to analyze sound and carious dentine regarding ester groups and their reaction with hydrazine based stains by means of Fourier Transform Infrared Spectroscopy (FTIR), Time of Flight Secondary Ion Mass Spectrometry (ToF-SIMS) light microscopy analysis and Nuclear magnetic resonance (NMR). Finally, to evaluate if chemo-mechanical excavation is effective in removal of these known alterations in carious tissue.

It can be concluded that:

- The FTIR absorption spectra showed that the carious tissue contained ester groups, not detected in sound dentine. The results also indicated a higher occurrence of ester groups in the inner layers of carious dentine than in the outer layer.
- Binding to these ester groups by hydrazine derivative was observed after different chemical treatments with FTIR-ATR, ToF-SIMS, solid-state  $^{13}\text{C}$  NMR and solid state  $^{15}\text{N}$  NMR spectroscopy.
- It was confirmed that  $^{15}\text{N}_2$ -hydrazine and  $^{15}\text{N}_2$ -labelled Lucifer yellow both bind to carious dentine but not to healthy dentine forming reaction products like acyl hydrazine or diacyl hydrazine.
- Based on the chemical and light-stereomicroscopic observations, dyes with covalently binding capacity were found to bind to carious dentine in a selective way in contrast to dyes with only electrostatic binding capacity.
- The systematic review and meta-analysis indicate, with causative interpretation, that the clinical efficacy of chemo-mechanical removal with Carisolv seems as reliable as the rotary instruments.



## 6 FINAL REMARKS

### **Clinical implications**

There is a variety among dentists to which extend different dyes are used during the excavation procedure. The products found on the market are from what is known today not selective, but still considered helpful by many. This series of studies have shown that there is a more specific staining may take place. It is the hope that this will improve the caries excavation step, minimize the removal of healthy tooth substance and increase the longevity of the filling as well as reduce risk for negative side effects of the tooth. Therefore optimising the observed reaction into clinical acceptable application will be a future prospective. In addition initial studies showed that these types of stains are compatible with chemo-mechanic excavation (Carisolv) and may offer a possibility to improve the minimal invasive methods that hopefully could be a part of reimbursement system.

To conclude, there seems to be an opportunity to improve the concept of minimal invasive dentistry but more studies are needed to evaluate this technique at its long-term effect in the clinic.

### **Molecular insight**

Much more work is needed in order to understand differences between sound and carious dentine on a molecular basis as well. Although our knowledge is far away from complete, new and sophisticated methods, such as solid state NMR increase the possibilities for future knowledge. Hence, the stable chemical changes in carious tissue describe the causative effects from the caries process that if understood can give more insights to why and how the process is initiated and further on how it may be inhibited. Knowledge contributing to define the molecular structure will therefore gain the patient, dentist and the society including a more tissue friendly treatment and a more cost-effective preventive and restorative handling. Another application of our

findings would be to place these alterations in a more detailed picture of the already described zones of a caries progression lesion. We found the esters to have a higher occurrence in the inner layer of carious dentine than in the outer layer. Esters are also expected to be present in the inner carious layer reaching the transparent zone, since bacteria is not the only requirement in forming esters. Thus it would be interesting to position them into the previous knowledge of the different zones of the lesion. However there will never be a clear line between judged area and / or presented zones in an infected biological tissue.

# ACKNOWLEDGEMENT

Mycket vatten har runnit under broarna innan denna avhandling till slut färdigställdes. Jag skulle vilja tacka så många, men det inte finns tillräckligt med textutrymme. Några individer har dock varit med under hela resan.

Peter Lingström, huvudhandledare; Du har medverkat till mina studier/projekt sedan min licentiatexamen och alltid varit uppmuntrande, även till lite tokiga idéer. Tack för allt ditt stöd, men framförallt för våra givande vetenskapliga diskussioner som alltid resulterat i intressanta projekt och publikationer. Tack för ett givande samarbete.

Åke Nilsson, bihandledare; utan dig hade inget av detta blivit av. Tusen tack! Och tack för att Du lyssnade och trodde på mig när jag för första gången frågade om en möjlig esterprocess, Äntligen.

Ett stort tack till alla medförfattare på samtliga delarbeten; Gedigna arbeten, med mycket tid och kunskap som insats. Arbetena har blivit lättfattliga och strukturerade. Tack för ett gott samarbete

Avdelningen för Cariologi; Tack för alla trevliga och givande samtal, speciellt vid lunch bordet.

Vänner och kollegor; Utan vänner står sig livet slätt. Tack Anna Lundgren, Karin Bergqvist, Therese Magnusson och Sara Lilliehöök. Ni vet vad Ni betyder. Utan duktiga och pålitliga kollegor är det svårt att utföra kvalificerat arbete. Tack till alla medarbetare på RLS, ifrån tidigare MediTeam, och många kvalificerade medarbetare på Chalmers. Ett speciellt tack till Louise Tottie som jag fått glädjen av att arbeta nära. En del av denna avhandling återfinns även i våra alster. Rolf Bornstein i vått och torrt, men så har de också blivit en hel del konkreta projekt. Eva Sheingold, Du har betytt mycket för mig och projektet.

Tack till Vinnova och VGR som i omgångar delfinansierat dessa studier ihop med RLS Global AB. Ett varmt tack för stödet; Vinnova (200901575; 201100942) och Västra Götaland Region (FoU kortet, RUN 652-0889-09).

Sist men inte minst ett varmt tack till de närmaste, min familj och släkt; Tack Jonas, Emil och Noah för att Ni orkade stå ut. Ni är bäst. Mamma och Pappa som alltid kommer att vara just "mamma och pappa" utan Er hade inget blivit av eller hur? Faster Assi, nu är det över! Tack syskon, svärföräldrar och övrig släkt för att Ni orkat lyssna på alla dessa detaljer.



# REFERENCES

1. Fejerskov O. Changing paradigms in concepts on dental caries: consequences for oral health care. *Caries Res* 2004; 38:182-91.
2. WHO. World Health Organization. Oral Health. Fact sheet No. 318 April; 2012 Available at: <http://www.who.int/mediacentre>
3. Marcenes W, Kassebaum NJ, Bernabé E, Flaxman A, Naghavi M, Lopez A, Murray CJ. Global burden of oral conditions in 1990-2010: a systematic analysis. *J Dent Res* 2013; 92:592-7.
4. Antunes JL, Narvai PC, Nugent ZJ. Measuring inequalities in the distribution of dental caries. *Community Dent Oral Epidemiol* 2004; 32:41-8.
5. SoS. Socialstyrelsen. Karies hos barn och ungdomar. Epidemiologiska uppgifter för år 2014. Artikelnummer 2015-11-36; 2015.
6. Selwitz RH, Ismail AI, Pitts NB. Dental caries. *Lancet* 2007; 369:51-9.
7. Marsh PD. Dental plaque as a biofilm and a microbial community - implications for health and disease. *BMC Oral Health* 2006; 15: 6, Suppl 1: 1-6.
8. Lingström P, Imfeld T, Birkhed D. Comparison of three different methods for measurement of plaque- pH in humans after consumption of soft bread and potato chips. *J Dent Res* 1993; 72:865-70.
9. Bratthall D, Hänsel-Petersson G, Sundberg H. Reason for the caries decline: what do the experts believe? *Eur J Oral Sci* 1996; 104:416-25, 430-2.
10. Marthaler TM. Changes in dental caries 1953-2003. *Caries Res* 2004; 38:173-81.
11. Black GV. A work on operative dentistry. Vol 1, The technical procedures in filling teeth. Chicago: Medico-Dental Publishing Co.1914.
12. Deligeorgi V, Mjör IA, Wilson NH. An overview of reasons for the placement and replacement of restorations. *Prim Dent Care* 2001;8:5-11.
13. Ericson D. The concept of minimally invasive dentistry. *Dent Update* 2007; 34:1: 9-10, 12-14, 17-18.

14. Marsh PD, Takahashi N, Nyvad B. Biofilms in caries development. In: Dental caries the disease and its clinical management. (3<sup>rd</sup> edn). Fejerskov O, Nyvad B, Kidd E. (Editors). Wiley Blackwell: Oxford; 2015 pp. 107-129.
15. Bowen WH, Koo H. Biology of streptococcus mutans-derived glucosyltransferases: role in extracellular matrix formation of cariogenic biofilms. *Caries Res* 2011; 45:69-86.
16. Borgström MK, Sullivan A, Granath L, Nilsson G. On the pH-lowering potential of lactobacilli and mutans streptococci from dental plaque related to the prevalence of caries. *Community Dent Oral Epidemiol.* 1997; 25:165-9.
17. Takahashi N, Nyvad B. The role of bacteria in the caries process: ecological perspectives. *J Dent Res* 2011; 90:294-303.
18. Alia-Garcia E, Parra-Pecharroman D, Sanchez-Diaz A, Mendez S, Royuela A, Gil-Alberdi L. Forensic identification in teeth with caries. *Forensic Sci Int* 2015; 257:236-41.
19. LeGeros RZ. Chemical and crystallographic events in the caries process. *J Dent Res* 1990; 69:(567-74):634-6.
20. Silwood CJ, Lynch EJ, Seddon S, Sheerin A, Claxson AW, Grootveld MC. <sup>1</sup>H-NMR analysis of microbial-derived organic acids in primary root carious lesions and saliva. *NMR Biomed* 1999; 12:6:345-56.
21. Geddes D. Acids produced by human dental plaque metabolism in situ. *Caries Res* 1975; 9:98-100.
22. Beighton D. The complex oral microflora of high-risk individuals and groups and its role in the caries process. *Community Dent Oral Epidemiol* 2005; 33:248-55.
23. Devulapalle KS, Gomez de Segura A, Ferrer M, Alcade M, Mooser G, Plou FJ. Effect of carbohydrate fatty acids esters on streptococcus sobrinus and glucosyltransferase activity. *Carbohydr Res* 2004; 339:1029-103.
24. Georgios A, Vassiliki T, Sotirios K. Acidogenicity and acidurance of dental plaque and saliva sediment from adults in relation to caries activity and chlorhexidine exposure. *J Oral Microbiol* 2015; 7:26197.
25. Lingström P, van Ruyven FO, van Houte J, Kent R. The pH of dental plaque in its relation to early enamel caries and dental plaque flora in humans. *J Dent Res* 2000; 79:770-7.
26. Di Renzo M, Ellis TH, Sacher E, Stangel I. A photoacoustic FTIR-study of the chemical modifications of human dentine surfaces: I. Demineralization. *Biomaterials* 2001; 22:787-92.

27. van Strijp AJ, van Steenberg T, de Graaff J, ten Cate JM. Bacterial colonization and degradation of demineralized dentin matrix in situ. *Caries research*. 1994; 28:21-7.
28. Silverstone LM. Laboratory studies on the demineralization and remineralization of human enamel in relation to caries mechanisms. *Aust Dent J* 1980; 25:163-8.
29. Eisenmann DR. Enamel structure. In: Oral histology development, structure and function. (4<sup>th</sup> edn). Ten cate Ar (Editor). Mosby. Inc: St. Louis, Missouri, USA; 1994
30. Goldberg M, Septier D, Lecolle S, Chardin H, Quintana MA, Acevedo AC. Dental mineralization. *Int J Dev Biol*. 1995; 39:93-110.
31. Nancy A. Development, structure and function. In Ten Cate's Oral histology. (7<sup>th</sup> edn). Ten Cate Ar (Editor). Mosby. Inc: St. Louis, Missouri, USA; 2013
32. Aizawa M, Matsuura T, Zhuang Z. Syntheses of single-crystal apatite particles with preferred orientation to the a- and c-axes as models of hard tissue and their applications. *Biol Pharm Bull* 2013; 36:11:1654-61.
33. Fejerskov O. Pathology of dental caries. In: Dental caries the disease and its clinical management. (3<sup>rd</sup> edn). Fejerskov O, Nyvad B, Kidd E. (Editors). Wiley Blackwell: Oxford; 2015 pp. 51-58.
34. Fejerskov O, Larsen MJ. Demineralisation and remineralisation: the key to understanding clinical manifestations of dental caries. In: Dental caries the disease and its clinical management. (3<sup>rd</sup> edn). Fejerskov O, Nyvad B, Kidd E. (Editors). Wiley Blackwell: Oxford; 2015 pp. 156-7.
35. van Loveren C, Lingström P. Diet and dental caries In: Dental caries the disease and its clinical management. (3<sup>d</sup> edn). Fejerskov O, Nyvad B, Kidd E. (Editors). Wiley Blackwell: Oxford; 2015 pp. 137..
36. Uskokovic V. Amelogenin in Enamel Tissue Engineering. *Adv Exp Med Biol* 2015; 88:1237-54
37. Castiblanco GA, Rutishauser D, Ilag LL, Martignon S, Castellanos JE, Mejia W. Identification of proteins from human permanent erupted enamel. *Eur J Oral Sci* 2015; 123:390-5.
38. Linde A. Dentin matrix proteins: composition and possible functions in calcification. *Anat Rec* 1989; 224:154-166
39. Butler WT. Dentine collagen: chemical structure and role in mineralization. In: Dentine and dentinogenesis. Linde A (Editor). CRC Press: Boca Raton, Florida; 1984 pp. 37-53.

40. Fujisawa R, Kuboki Y. High resolution solid-state nuclear magnetic resonance spectra of dentine collagen. *Biochem Biophys Res Commun* 1990; 167:761-6.
41. Becker J, Schuppan D, Benzian H, Bals T, Hahn EG, Cantaluppi C, Reichart P. Immunohistochemical distribution of collagen types IV, V, and VI and of pro-collagens types I and III in human alveolar bone and dentin. *J Histochem Cytochem* 1986; 34:11: 1417-29.
42. Waltimo J, Risteli L, Risteli J, Lukinmaa PL. Altered collagen expression in human dentine: increased reactivity of type III and presence of type VI in dentinogenesis imperfecta, as revealed by immunoelectron microscopy. *J Histochem Cytochem* 1994; 42: 1593-601.
43. Karjalainen S, Soderling E, Pelliniemi L, Foidart JM. Immunohistochemical localization of types I and III collagen and fibronectin in the dentin of carious human teeth. *Arch Oral Biol*. 1986; 31:801-6.
44. Linde A, Goldberg M. Dentinogenesis. *Crit Rev Oral Biol Med* 1993; 4:679-728.
45. Almhöjd-Scherdin U. Chemical Alterations in Dental Caries An Experimental Study of Collagen with Mass Spectrometry (MALDI-TOF & LTQ-FT-MS/MS). Thesis (Degree of Licentiate of Philosophy); 2006
46. Butler WT, Ritchie H. The nature and functional significance of dentin extracellular matrix proteins. *Int J Dev Biol* 1995; 39:169-79.
47. Boskey AL. Noncollagenous matrix proteins and their role in mineralization. *Bone Miner* 1989; 6:111-23.
48. Glimcher MJ. Recent studies of the mineral phase in bone and its possible linkage to the organic matrix by protein-bound phosphate bonds. *Philos Trans R Soc Lond B Biol Sci*. 1984; 304:479-508.
49. Duer MJ, Frisic' T, Murray RC, Reid DG, Wise ER. The mineral phase of calcified cartilage: Its molecular structure and interface with organic matrix. *Biophys J* 2009; 96:3372-3378
50. Veis A, Eggenberger DN, Cohen J. The degradation of collagen III. Characterization of soluble products of mild acid degradation. *Am. Chem. Soc.* 1955; 77:2368-74.
51. Veis A, Perry A. The phosphoprotein of dentin matrix. *J Biochem*. 1967; 6:2409-16.
52. Dung TS-Z, Li Y, Dunipace AJ, Stookey GK. Degradation of insoluble bovine collagen and human dentine collagen pretreated

- in vitro* with lactic acid, pH 4.0 and 5.5. Arch Oral Biol 1994; 39:10: 901 - 905.
53. Gotliv BA, Veis A. The composition of bovine peritubular dentin: matching TOF-SIMS, scanning electron microscopy and biochemical component distributions. New light on peritubular dentin function. Cells Tissues Organs 2009; 189:12-19.
  54. Goldberg M, Kulkarni AB, Young M, Boskey A. Dentin: structure, composition and mineralization. Frontiers in bioscience. 2011; 3:711-35.
  55. Fejerskov O, Nyvad B. Clinical features of caries lesions Dental In: Dental caries the disease and its clinical management. (3<sup>d</sup> edn). Fejerskov O, Nyvad B, Kidd E. (Editors) Wiley Blackwell: Oxford; 2015 pp. 11-13.
  56. Fejerskov O, Nyvad B, Kidd EAM. Dental caries: what is it? In: Dental caries the disease and its clinical management. (3<sup>d</sup> edn). Fejerskov O, Nyvad B, Kidd E. (Editors). Wiley Blackwell: Oxford; 2015 pp. 7-10.
  57. Mjör A. The morphology of dentine and dentinogenesis. In: Dentin and dentinogenesis. Linde A (Editor). CRC Press Inc: Boca Raton Florida; 1994 pp. 351-353.
  58. Fusayama T. Two layers of carious dentin; diagnosis and treatment. Operative Dentistry. 1979; 4: 63-70.
  59. Fusayama T, Okuse K, Hosoda H. Relationship between hardness, discoloration and microbial invasion in carious dentine. J Dent Res. 1996;45:1033-46.
  60. Kidd EA, Ricketts DN, Beighton D. Criteria for caries removal at the enamel-dentine junction: a clinical and microbiological study. Br Dent J. 1996;180:287-91.
  61. Ohgushi K, Fusayama T. Electron microscopic structure of the two layers of carious dentin. J Dent Res. 1975; 54: 1019-26.
  62. Kuboki Y, Ohgushi K, Fusayama T. Collagen biochemistry of the two layers of carious dentine. J Dent Res 1977; 56:1233-7.
  63. Pugach M, Strother K, Darling J, Fried CL, Gansky SA, Marshall SJ, Marshall GW. Dentin caries zones: mineral, structure, and properties. J Dent Res 2009; 88: 71-6.
  64. Kidd EA. Clinical threshold for carious tissue removal. Dent Clin North Am 2010; 54:541-9.
  65. Ogawa K, Yamashita Y, Ischj T, Fusayama T. The ultrastructure and hardness of the transparent layer of human carious dentine. J Dent Res 1983; 62:7-10.

66. Liu Y, Yao X, Liu YW, Wang Y. A Fourier transform infrared spectroscopy analysis of carious dentin from transparent zone to normal zone. *Caries Res* 2014; 48:320-9.
67. Armstrong WG. Chemistry of carious enamel and dentine. *J Dent Res*. 1964; 43:1002-6.
68. Armstrong WG. Modifications of the properties and composition of the dentin matrix caused by dental caries. *Adv Oral Biol*. 1964; 42:309-32.
69. Kleter GA, Damen JJ, Buijs MJ, Ten Cate JM. The maillard reaction in demineralized dentine in vitro. *Eur J Oral Sci*. 1997; 105:278-280.
70. Kleter GA, Damen JJ, Buijs MJ, Ten Cate JM. Modification of amino acid residues in carious dentin matrix. *J Dent Res*. 1998; 77:488-495.
71. Thylstrup A, Braun C, Holmen L. In vitro caries models – mechanisms for caries initiation and arrestment. *Adv Dent Res* 1994; 8:144-57.
72. Spencer P, Wang Y, Katz JL, Misra A. Physicochemical interactions at the dentine/adhesive interface using FTIR chemical imaging. *J Biomed Opt* 2005; 10: (031104)-1-11
73. Kidd EA. How ‘clean’ must a cavity be before restoration? *Caries Res* 2004; 38: 305-313.
74. Marshall GW Jr, Marshall SJ, Kinney JH, Balooch M. The dentin substrate: structure and properties related to bonding. *J Dent*. 1997; 25:441-58.
75. Gotliv BA, Veis A. Peritubular dentin, a vertebrate apatitic mineralized tissue without collagen: role of a phospholipid-proteolipid complex. *Calief Tissue Int*. 2007; 81:191-205.
76. Zavgorodnty AV, Rohanizadeh R, Swain MV. Ultra structure of dentine carious lesions. *Arch Oral Biol*. 2008; 53:124-132.
77. Tian SF, Toda S, Higashino H, Matsumura S. Glycation decreases the stability of the triple-helical strands of fibrous collagen against proteolytic degradation by pepsin in a specific temperature range. *J Biochem* 1996; 120:6:1153-62.
78. Larmas MA. Chromatographic and histochemical study of non-specific esterases in human carious dentine. *Arch Oral Biol*. 1972; 17:1121-32.
79. Dirksen TR. Lipid components of sound and carious dentine. *J Dent Res*. 1963; 42:128-32.
80. Carey FA, Sundberg JR (Editors). *Advanced organic chemistry*. (3<sup>d</sup>edn). New York: Plenman Press; 1990

81. Watson WT, Minogue TD, Val DL, Beck von Bodman S, Mair E.A. Structural asis and specificity of acyl-homoserine lactone signal production in bacterial quorum sensing *Mol. Cell* 2002; 9:685–694.
82. Swift S, Downie JA, Whitehead NA, Barnard AM, Salmond GP, Williams P. Quorum sensing as a population-density-dependent determinant of bacterial physiology. *Adv Microb Physiol.* 2001; 45:199-270.
83. Kuboki J, Liu CF, Fusayama T. Mechanism of differential staining in carious dentine *Dent Res.* 1983; 62:713-4.
84. van de Rijke JW: Use of dyes in cariology *Int Dent J* 1991; 41:111-116.
85. Hosoya Y, Taguchi T, Tay FR. Evaluation of a new caries detecting dye for primary and permanent carious dentine *J Dent* 2007; 35:137-143.
86. Rodrigues J, Neuhaus K, Diniz BM, Hug I, Stich H, Karlsson L, Lussi A. Comparison among gold standard techniques used for the validation of methods for occlusal caries detection *Micros Res Tech* 2012; 75: 605-608.
87. Zavareh FA, Yazdizadeh M. Comparison of conventional detection and caries detector dye. *J Biol Sci* 2008; 3:1067-69.
88. Itoh K, Kusunoki M, Oikawa M, Tani C. In vitro comparison of three caries dye. *Am J Dent.* 2009; 22:195.
89. Franco SJ, Kelsey WP. Caries removal with and without a disclosing solution of basic fuchine. *Oper Dent.* 1981; 6:46-8.
90. de Almeida Neves A, Coutinho E, Cardoso MV, Lambrechts P, van Meerbeek B. Current concepts and techniques for caries excavation and adhesion to residual dentin. *J Adhes Dent* 2011; 13:7-22.
91. Boston DW, Jefferies SR, Gaughan JP. The relative location of the dye staining endpoint indicated with polypropylene glycol-based Caries Dye versus Conventional Propylene Glycol-Based Caries Dye. *Eur J Dent* 2008; 2:29-36
92. Boston DW, Liao J. Staining of non-carious human coronal dentin by caries dyes. *Oper Dent.* 2004; 29:280-286.
93. Javaheri M, Maleki-Kambakhsh S, Etemad-Moghadam Sh. Efficacy of two caries detector dyes in the Diagnosis of Dental Caries *J Dent Tehran* 2010; 7:71-6.
94. Boston DW, Graver HT. Histological study of an acid red caries-disclosing dye. *Oper Dent.* 1989; 14:186-192.

95. Anderson MH, Charbeneau GT. A comparison of digital and optical criteria for detecting carious dentin *J Prosthet Dent* 1985; 53:643-646.
96. Yip HK, Stevenson AG, Beeley JA. The specificity of caries detector dyes in cavity preparation. *Br Dent J* 1994; 176: 417-21.
97. Kidd EA, Joyston-Bechal S, Beighton D. The use of a caries detector dye during cavity preparation: a microbiological assessment. *Br Dent J* 1993; 174:245-48.
98. Lennon AM, Attin T, Buchalla W. Quantity of remaining bacteria and cavity size after reexcavation with FACE, caries detector dye and conventional excavation *In Vitro. Oper Dent* 2007; 32-3: 236-41.
99. Mollica FB, Rocha Gomes Torres C, Goncalves SE, Mancini MN. Dentine microhardness after different methods for detection and removal of carious dentine tissue. *J Appl Oral Sci* 2012; 20:4:449-54.
100. McComb, D. Caries-detector dyes how accurate and useful are they? *J Can Dent Assoc* 2000; 66:195-8.
101. Yasukawa A, Yokoyama T, Kandori K, Ishikawa T. Ion-exchange of magnesium-calcium hydroxyapatite solid solution particles with Cd<sup>2+</sup> ion. *Colloids and Surfaces A: Physicochemical and Engineering Aspects*. 2008; 317:123-128.
102. March J. Reactions, Mechanisms and Structure. In March J (ed). *Advanced Organic Chemistry*. (4<sup>th</sup> edn.) Wiley: New York; 1992 pp 421-427 and 904-908.
103. Banerjee A, Kidd EA, Watson TF. In vitro evaluation of five alternative methods of carious dentine excavation. *Caries Res* 2000; 34:144-150.
104. Ericson D, Zimmerman M, Raber H, Götrick B, Bornstein R, Thorell J. Clinical evaluation of efficacy and safety of a new method for chemo-mechanical removal of caries. A multi-centre study. *Caries Res* 1999; 33:171-77.
105. Hannig M. Effect of Carisolv<sup>TM</sup> solution on sound, demineralized and denatured dentin - an ultrastructural investigation. *Clin Oral Invest* 1999; 3:155-159.
106. Wennerberg A, Sawase T, Kultje C. The influence of Carisolv<sup>TM</sup> on enamel and dentine surface topography. *Eur J Oral Sci* 1999; 107: 297-306.
107. Arvidsson A, Liedberg B, Moller K, Lyven B, Sellen A, Wennerberg A. Chemical and topographical analyses of dentine surfaces after Carisolv treatment. *Journal of dentistry*. 2002; 30:2-3:67-75

108. Tonami K, Araki K, Mataka S, Kurosaki N. Effects of chloramines and sodium hypochlorite on carious dentin. *J Med Dent Sci* 2003; 50:139-146.
109. Morrow LA, Wilson NH, Watts DC, Silikas N. The nature of the remaining dentin surface following application of Carisolv solution. *Am J Dent* 2005;18:296-300.
110. Pai VS, Nadig RR, Jagadeesh T, Usha G, Karthik J, Sridhara K. Chemical analysis of dentin surfaces after Carisolv treatment. *J Conserv Dent* 2009; 12:118-22.
111. Soni HK, Sharma A, Sood, PB. A comparative clinical study of various methods of caries removal in children. *Eur Arch Paediatr Dent*. 2015; 16:19-26.
112. Keenan AV, Congiusta, MA. Efficacy of using Carisolv in the removal of decayed tooth structure in primary teeth. *Evid Based Dent* 2016; 17:2:44-5.
113. Baker RWR. Studies on the reaction between sodium hypochlorite and proteins. *Biochem* 1947; 41:23:337-342.
114. Kantouch A, Abdel-Fattah SH. Action of sodium hypochlorite on  $\alpha$ -amino acids. *Chem Zvesti*. 1971; 25:222-30.
115. Schutzbank SG, Galaini J, Kronman JH et al. A comparative in vitro study of the effect of GK-101 and GK 101E in caries removal. *J Dent Res*; 1978: 57: 861-4.
116. Thomas EL, Grisham MB, Jefferson MM. Preparation and characterization of chloramines. *Meth in Enzymology*. 1986b pp. 132: 569–85.
117. Hawkins CL, Pattison DL, Davies MJ. Hypochlorite-induced oxidation of amino acids, peptides and proteins. *Amino acids* 2003; 25:259-274.
118. Habib CM, Kronman J, Goldman M. A. chemical evaluation of collagen and hydroxyproline after treatment with GK-101 (N-chloroglycine). *Pharmacol Ther Den* 1975; 2:209-215.
119. Armesto XL, Canle ML, Santaballa JA. Amino acids chlorination in aqueous media. *Tetrahedron* 1993; 49: 275-284.
120. Peskina AV, Midwinter RG, Harwood DT, Winterboum CC. Chlorine transfer between glycine, taurine and histamine: reaction rates and impact on cellular reactivity. *Free Radic Biol Med* 2005; 38:397-405.
121. Takeuchi H, Matsushima K, Nishiyama N, Nemoto K, Tsujimoto Y. Free radical study using electron spin resonance and structural analysis by nuclear magnetic resonance of the Carisolv system. *Int J Oral Sci* 2015; 4:14-20.

122. Tawakoli PN, Ragnarsson KT, Rechenberg DK, Moln D, Zehnder M. Effect on endodontic irrigants on biofilm matrix polysaccharides. *Int Endo J*. 2017; 50:153-160.
123. Maru VP, Shakuntala BS, Nagarathna C. Caries Removal by Chemomechanical (Carisolv™) vs. Rotary Drill: A Systematic Review. *Open Dent J* 2015; 31:462-72.
124. Fure S, Lingstrom P. Evaluation of the chemomechanical removal of dentine caries in vivo with a new modified Carisolv gel. *Clin Oral Investig* 2004; 8:139-44.
125. Fure S, Lingstrom P, Birkhed D. Evaluation of Carisolv for the chemo-mechanical removal of primary root caries in vivo *Caries Res* 2000; 34:3: 275-80.
126. Schwendicke F, Paris S, Tu YK. Effects of using different criteria for caries removal: a systematic review and network meta-analysis. *J Dent* 2015; 43:1-15.
127. Li R, Zhao Y, Ye L. How to make choice of the carious removal methods, Carisolv or traditional drilling? A meta-analysis. *J Oral Rehabil* 2014; 41:432-42.
128. Marquezan M, Faraco Junior I M, Feldens CA, Tovo MF, Ottoni AB. Evaluation of the methodologies used in clinical trials and effectiveness of chemo-mechanical caries removal with Carisolv. *Braz Oral Res* 2006; 20:364-71.
129. Scott PG, Leaver AG. The degradation of human dentine collagen by trypsin. *Conn Tissue Res* 1974; 2: 299 - 307.
130. Hynes A, Scott AD, Man A, Singer DL, Sowa MG, Liu KZ. Molecular mapping of periodontal tissues using infrared microspectroscopy. *BMC Med Imaging* 2005; 5:1-10.
131. Boskey A, Pleshko Camacho N. FT-IR imaging of native and tissue-engineered bone and cartilage. *Biomaterials* 2007; 28:2465-78.
132. Dickinson ME, Wolf KV, Mann AB. Nanomechanical and chemical characterization of incipient in vitro carious lesions in human dental enamel. *Arch Oral Biol*. 2007; 52:753-760.
133. Nam, 2015, Nam JW, Phansalkar RS, Lankin DC, Bisson J, McAlpine JB, Leme AA, Vidal CM, Ramirez B, Niemitz M, Bedran-Russo A, Chen SN, Pauli GF: Chemical shifts explain the NMR fingerprints of oligomeric proanthocyanidins with high dentin biomodification potency. *J Org Chem* 2015; 80:7495-7507.
134. Ni Q, Chen S: Assessment of structural changes of human teeth by low-field nuclear magnetic resonance (NMR). *Meas Sci Technol* 2010; 21:15803.

135. Banerjee A, Watson TF, Kidd EA. Dentine caries: take it or leave it? *Dental Update* 2000; 27: 272-6.
136. Sturdevant CM, Barton RE, Sockwell CL. In: *Sturdevant's Art and Science of Operative Dentistry*. (2<sup>nd</sup> edn). Roberson T, Heymann HO, Swift Jr EJ. (Editor). Mosby: St. Louis C. V; 1984 pp. 35-63.
137. Silverstein RM, Clayton Bassler G, Morill TC, Sawicki D (Editors). *Spectrometric identification of organic compounds*. (5<sup>th</sup> edn). John Wiley & sons Inc: New York; 1991.
138. Benninghoven, A. *Chemical Analysis of Inorganic and Organic Surfaces and Thin Films by Static Time-of-Flight Secondary Ion Mass Spectrometry (TOF-SIMS)*. *Angew Chem Int Ed Eng*. 1994; 33:1023-43.
139. Chittur KK. FTIR/ATR for protein adsorption to biomaterial surfaces. *Biomaterial* 1998; 19:4-5:357-69.
140. Harris DC, Lucy CA. (Editors). *Quantitative chemical analysis*. (9<sup>th</sup> edn). WH Freeman and company: New York; 2016
141. Spool A. The practice of ToF-SIMS Time of flight secondary ion mass. In: *Materials characterisation and analysis collection*. CR Brundle (Editor). Momentum press LLC: New York; 2016
142. Gamble, L. J. Anderton, C. R. *Secondary Ion Mass Spectrometry Imaging of Tissues, Cells, and Microbial Systems*. *Micros Today* 2016; 24:24-31.
143. Friebolin H (Editor). *Basic one-and two –dimensional NMR Spectroscopy*. (2<sup>nd</sup> edn). VCH publisher: Weinheim DE; 1993
144. Fritz S, Meyer B *Electrochemical solid state analysis: state of the art*. *Chem Soc Rev* 1994; 23: 341-347.
145. Laws DD, Bitter HM, Jerschow A. Solid-state NMR spectroscopic methods. In *chemistry Angew Chem Int Ed Engl*. 2002; 41:3096-129.
146. Almhöjd U, Norén JG, Nilsson Å, Lingström P. Different methods for excavation and staining of caries-infected tissue. Abstract ID 180154. IADR, 46<sup>th</sup> September 4-7, 2013, Florence, Italy
147. Moher D, Liberati A, Tetzlaff J, Altman DG. Preferred reporting items for systematic reviews and meta-analyses: The PRISMA statement. *PLoS Med*. 2009; *PLoS Med* 2009;6:e1000097.
148. Hojo S, Komatsu M, Okuda R, Takahashi N, Yamada, T. Acid profiles and pH of carious dentin in active and arrested lesions. *J Dent Res*. 1994; 73: 1853-7.
149. Kahn CB, Hollander JL, Schumacher HR. Corticosteroid crystals in synovial fluid. *Jama* 1970; 211:5:807-9.
150. Dickens F, Jones HE. Carcinogenic activity of series of reactive lactones ad related substances. *Br J Cancer* 1961; 15:85-100.

151. Potter K, Kidder LH, Levin IW, Lewis EN, Spencer RG. Imaging of collagen and proteoglycan in cartilage sections using fourier transform infrared spectral imaging. *Arthritis Rheum* 2001; 44:846-55.
152. Schulz J, Pretzsch M, Khalaf I, Deiwick A, Scheidt HA, Salis-Soglio G, Bader A, Huster D. Quantitative monitoring of extracellular matrix production in bone implants by  $^{13}\text{C}$  and  $^{31}\text{P}$  solid-state nuclear magnetic resonance spectroscopy. *Calcif Tissue Int* 2007; 80:275-285.
153. Kolosowski KP, Sodhi RN, Kisen A, Basrani BR. Qualitative analysis of precipitate formation on the surface and in the tubules of dentin irrigated with sodium hypochlorite and a final rinse of chlorhexidine or QMiX. *J Endod* 2014; 40:2036-2040.
154. Dos A, Schimming V, Tosoni S, Limbach HH. Acid-base interactions and secondary structures of poly-L-lysine probed by  $^{15}\text{N}$  and  $^{13}\text{C}$  solid state NMR and Ab initio model calculations. *J Phys Chem B* 2008; 112:15604-15.
155. Fritz H, Kristinsson H, Mollenkopf M, Winkler T.  $^{15}\text{N}$  and  $^{13}\text{C}$  study of acylated hydrazines. The instability of trifluoroacetylhydrazide in the solid state. *Magn Reson Chem.* 1990; 28:331-336.
156. Preece NE, Nicholson JK, Timbrell JA. Identification of novel hydrazine metabolites by  $^{15}\text{N}$ -NMR. *Biochem Pharmacol* 1991; 41:1319-24.